



**HAL**  
open science

## Gut microbiota-derived short-chain fatty acids regulate IL-17 production by mouse and human intestinal $\gamma\delta$ T cells

Louise Dupraz, Aurélie Magniez, Nathalie Rolhion, Mathias L Richard, Grégory da Costa, Sothea Touch, Camille Mayeur, Julien Planchais, Allison Agus, Camille Danne, et al.

### ► To cite this version:

Louise Dupraz, Aurélie Magniez, Nathalie Rolhion, Mathias L Richard, Grégory da Costa, et al.. Gut microbiota-derived short-chain fatty acids regulate IL-17 production by mouse and human intestinal  $\gamma\delta$  T cells. Cell Reports, 2021, 36 (1), pp.109332. 10.1016/j.celrep.2021.109332 . hal-03282473

HAL Id: hal-03282473

<https://hal.sorbonne-universite.fr/hal-03282473v1>

Submitted on 9 Jul 2021

**HAL** is a multi-disciplinary open access archive for the deposit and dissemination of scientific research documents, whether they are published or not. The documents may come from teaching and research institutions in France or abroad, or from public or private research centers.

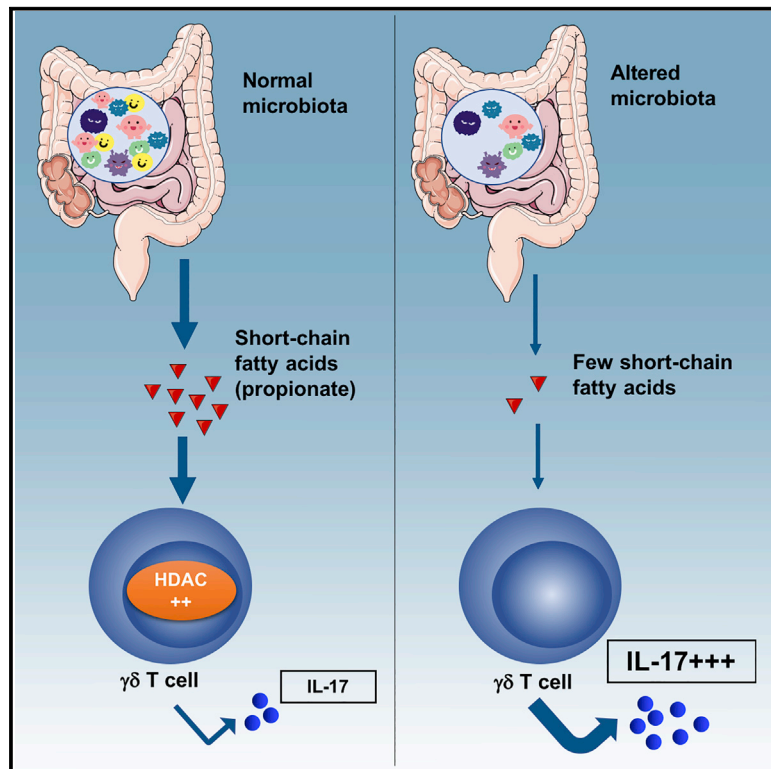
L'archive ouverte pluridisciplinaire **HAL**, est destinée au dépôt et à la diffusion de documents scientifiques de niveau recherche, publiés ou non, émanant des établissements d'enseignement et de recherche français ou étrangers, des laboratoires publics ou privés.



Distributed under a Creative Commons Attribution - NonCommercial - NoDerivatives 4.0 International License

# Gut microbiota-derived short-chain fatty acids regulate IL-17 production by mouse and human intestinal $\gamma\delta$ T cells

## Graphical abstract



## Authors

Louise Dupraz, Aurélie Magniez, Nathalie Rolhion, ..., Philippe Langella, Harry Sokol, Marie-Laure Michel

## Correspondence

marie-laure.michel@inrae.fr

## In brief

Dupraz et al. demonstrate that short-chain fatty acids, particularly propionate, reduce IL-17 production by mouse intestinal  $\gamma\delta$  T cells and human IL-17-producing  $\gamma\delta$  T cells from patients with inflammatory bowel disease (IBD). These microbiota-derived metabolites act directly on  $\gamma\delta$  T cells in a histone deacetylase-dependent manner.

## Highlights

- The gut microbiota represses IL-17 production by cecal  $\gamma\delta$  T cells
- Short-chain fatty acids repress IL-17- and IL-22-producing  $\gamma\delta$  T cells
- Propionate acts on  $\gamma\delta$  T cell functionalities by inhibiting histone deacetylase
- Propionate represses IL-17 production by human  $\gamma\delta$  T cells from patients with IBD



## Article

# Gut microbiota-derived short-chain fatty acids regulate IL-17 production by mouse and human intestinal $\gamma\delta$ T cells

Louise Dupraz,<sup>1,2</sup> Aurélie Magniez,<sup>1,3</sup> Nathalie Rolhion,<sup>2,3</sup> Mathias L. Richard,<sup>1,3</sup> Grégory Da Costa,<sup>1,3</sup> Sothea Touch,<sup>2,3</sup> Camille Mayeur,<sup>1,3</sup> Julien Planchais,<sup>1,3</sup> Allison Agus,<sup>1,3</sup> Camille Danne,<sup>1,3</sup> Chloé Michaudel,<sup>1,3</sup> Madeleine Spatz,<sup>1,3</sup> François Trottein,<sup>4</sup> Philippe Langella,<sup>1,3</sup> Harry Sokol,<sup>1,2,3</sup> and Marie-Laure Michel<sup>1,3,5,\*</sup>

<sup>1</sup>Université Paris-Saclay, INRAE, AgroParisTech, Micalis Institute, 78350 Jouy-en-Josas, France

<sup>2</sup>Sorbonne Université, INSERM, Centre de Recherche Saint-Antoine, CRSA, AP-HP, Saint-Antoine Hospital, Gastroenterology Department, 75012 Paris, France

<sup>3</sup>Paris Center for Microbiome Medicine (PaCeMM) FHU, Paris, France

<sup>4</sup>Centre d'Infection et d'Immunité de Lille, INSERM U1019, CNRS UMR 9017, University of Lille, CHU Lille, Institut Pasteur de Lille, 59000 Lille, France

<sup>5</sup>Lead contact

\*Correspondence: [marie-laure.michel@inrae.fr](mailto:marie-laure.michel@inrae.fr)  
<https://doi.org/10.1016/j.celrep.2021.109332>

## SUMMARY

Gut interleukin-17A (IL-17)-producing  $\gamma\delta$  T cells are tissue-resident cells that are involved in both host defense and regulation of intestinal inflammation. However, factors that regulate their functions are poorly understood. In this study, we find that the gut microbiota represses IL-17 production by cecal  $\gamma\delta$  T cells. Treatment with vancomycin, a Gram-positive bacterium-targeting antibiotic, leads to decreased production of short-chain fatty acids (SCFAs) by the gut microbiota. Our data reveal that these microbiota-derived metabolites, particularly propionate, reduce IL-17 and IL-22 production by intestinal  $\gamma\delta$  T cells. Propionate acts directly on  $\gamma\delta$  T cells to inhibit their production of IL-17 in a histone deacetylase-dependent manner. Moreover, the production of IL-17 by human IL-17-producing  $\gamma\delta$  T cells from patients with inflammatory bowel disease (IBD) is regulated by propionate. These data contribute to a better understanding of the mechanisms regulating gut  $\gamma\delta$  T cell functions and offer therapeutic perspectives of these cells.

## INTRODUCTION

The gut microbiota is a complex ecosystem essential for host defense against infection, nutrient metabolism, and tissue repair (Thursby and Juge, 2017). Since the last decade, many studies have described the profound effect of metabolites produced by commensal bacteria on immune cells such as dendritic cells (innate immunity) and conventional T lymphocytes (adaptive response). However, to mount rapid effector responses, the immune system also benefits from the local presence of  $\gamma\delta$  T cells (Chien et al., 2014). These innate T lymphocytes migrate early in their development toward epithelial surfaces and remain at these sites as resident cells. In the steady state,  $\gamma\delta$  T cells in the gut represent only a minor subset of interleukin-17A (IL-17)-producing T lymphocytes; upon infection by microorganisms such as *Listeria monocytogenes*, *Clostridium difficile*, or *Plasmodium falciparum*, these cells expand and make critical contributions to host defense (Sheridan et al., 2013; D'Ombra et al., 2007; Chen et al., 2020). Upon IL-23 and IL-1 $\beta$  stimulation,  $\gamma\delta$  T cells express the transcription factor retinoic acid-related orphan receptor (ROR)- $\gamma$ T and can produce IL-22.

$\gamma\delta$  T cells are known to protect the epithelial barrier (Workalemahu et al., 2003) but promote progression of colorectal cancer

in humans (Wu et al., 2014; Silva-Santos et al., 2015). Despite growing evidence of their implication in inflammatory bowel disease (IBD), such as Crohn disease (Hueber et al., 2012; McCarthy et al., 2013), their role remains unclear because they act both to protect against and induce inflammation. T cell receptor (TCR)  $\gamma\delta$ -knockout (KO) mice (deficient in  $\gamma\delta$  T cells) are more susceptible to dextran sodium sulfate (DSS)-induced colitis (Kühl et al., 2007), but  $\gamma\delta$  T cells have been shown to favor T helper 17 (Th17) differentiation and to enhance T cell-mediated colitis (Do et al., 2011). Hence, this population is a double-edged sword in intestinal inflammation and protection, and there is a need to identify factors that regulate their functions.

Previous studies have shown that antibiotics alter the  $\gamma\delta$  T cell compartment, implicating gut commensal bacteria in its expansion and/or maintenance in the gut lamina propria (Duan et al., 2010). Aryl hydrocarbon receptor (AhR) ligands, catabolized from tryptophan by the gut microbiota, are essential to maintain intraepithelial  $\gamma\delta$  T cells in the intestine (Li et al., 2011). However, the mechanisms of interaction between the gut microbiota and  $\gamma\delta$  T cells in the lamina propria remain obscure, and very few studies have explored how commensal bacteria regulate the pro- and anti-inflammatory properties of this population or which microbiota-derived metabolites can alter  $\gamma\delta$  T cell subset functionalities.



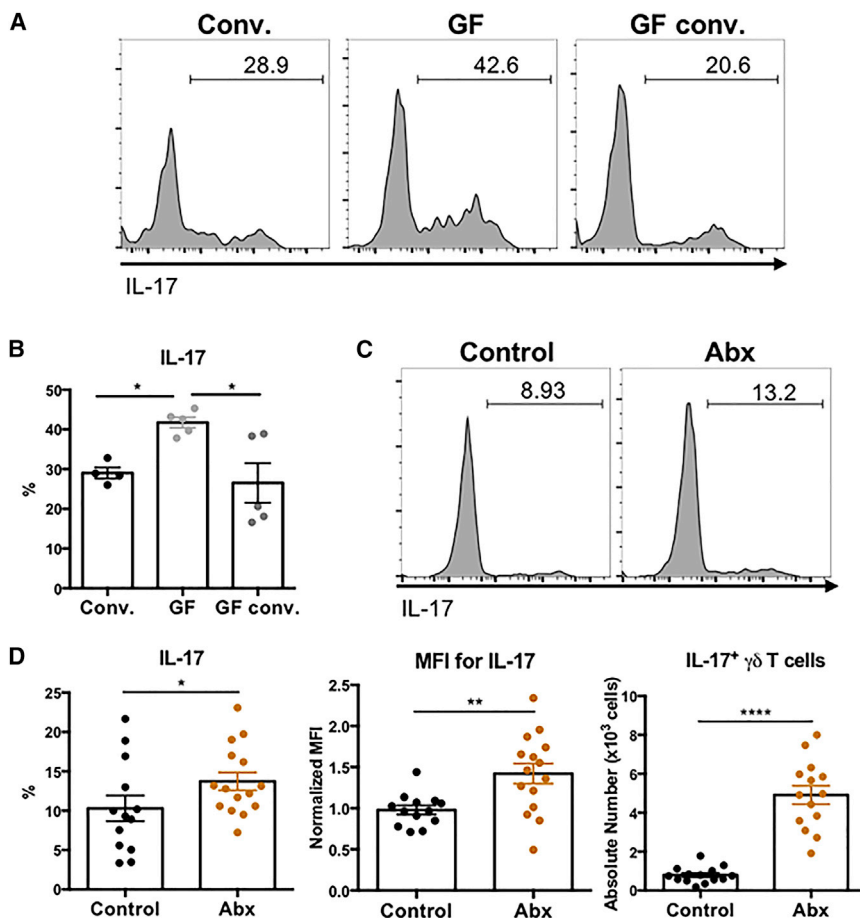


**Figure 1. The gut microbiota represses IL-17 production by cecal  $\gamma\delta$  T cells**

(A) Intracellular analysis of gated  $\gamma\delta$  T cells from cecum obtained from untreated conventional mice (conv.), germ-free mice (GF), and germ-free mice colonized with conventional mouse microbiota for 4 weeks (GF conv.).

(B) IL-17 production by cecal  $\gamma\delta$  T cells obtained as described in (A).

(C) Intracellular analysis of gated  $\gamma\delta$  T cells from cecum obtained from untreated mice (control) and broad-spectrum antibiotics-treated mice (Abx).

(D) IL-17 production (left) and normalized median fluorescence intensity (MFI) for IL-17 (middle) in gated  $\gamma\delta$  T cells and absolute number of IL-17<sup>+</sup>  $\gamma\delta$  T cells from cecum obtained as described in (C). In each case, cells were stimulated with phorbol 12-myristate 13-acetate (PMA) + ionomycin + IL-1 $\beta$  + IL-23 for 3 h. Errors bars are SEM from 4 to 5 mice (B) and from 13 to 15 mice (D) per group. Significant differences were determined using two-tailed Mann-Whitney test: \* $p < 0.05$ ; \*\* $p < 0.01$ ; \*\*\*\* $p < 0.0001$ . See also Figure S1.

(Duan et al., 2010; Cheng et al., 2014; Li et al., 2017). However, as was reported previously (Geddes et al., 2011), the proportion of IL-17<sup>+</sup>  $\gamma\delta$  T cells (gated as described in Figure S1A) is increased in the cecum of germ-free mice (Figures 1A and 1B; Figure S1B), suggesting that commensals possibly modulate  $\gamma\delta$  T cells differentially in this compartment. In contrast to conventional CD4<sup>+</sup> T cells,  $\gamma\delta$

T cells still produced IL-17 in sterile environments (Figure S1C). To determine whether the gut microbiota inhibits IL-17 production by cecal  $\gamma\delta$  T cells, germ-free mice were colonized with conventional mouse microbiota for 4 weeks. Although  $\gamma\delta$  T cells produced more IL-17 in germ-free mice than in conventional mice, the transfer of microbiota was sufficient to lower significantly the frequency of cecal IL-17-producing  $\gamma\delta$  T cells, together with a tendency toward a decreased number, and recapitulate the conventional mouse phenotype (Figures 1A and 1B; Figure S1B). In concordance with these results, broad-spectrum antibiotic treatment significantly increased the proportion and absolute number of IL-17<sup>+</sup>  $\gamma\delta$  T cells in the cecum lamina propria (Figures 1C and 1D; Figure S1D) and, more importantly, their production of IL-17 (Figure 1D).

Here, we show a dichotomy between small-bowel, cecal, and colonic IL-17- and IL-22-producing  $\gamma\delta$  T cells, with the gut microbiota regulating these three compartments differentially. While the gut microbiota stimulates the production of IL-17 and IL-22 by  $\gamma\delta$  T cells in the small intestine lamina propria, the opposite effect is observed in the colon and cecum. We next identified short-chain fatty acids (SCFAs), metabolites produced by the microbiota in the cecum and colon, as key regulators of IL-17 and IL-22 production by  $\gamma\delta$  T cells in the gut lamina propria. These metabolites, particularly propionate, which is produced by the gut microbiota in the cecum and colon, can directly affect  $\gamma\delta$  T cell functional properties by inhibiting histone deacetylase (HDAC) activity. Moreover, the production of IL-17 by human  $\gamma\delta$  T cells is inhibited by propionate. Collectively, our data reveal the crucial role of gut microbiota-derived SCFAs in regulating IL-17 and IL-22 production by  $\gamma\delta$  T lymphocytes, thus paving the way for microbiota-based therapies for diseases involving these cells.

## RESULTS

### The gut microbiota represses IL-17 production by cecal $\gamma\delta$ T cells

The gut microbiota is essential for maintaining IL-17-producing  $\gamma\delta$  T cells in the small intestine, peritoneum, liver, and lung

T cells still produced IL-17 in sterile environments (Figure S1C). To determine whether the gut microbiota inhibits IL-17 production by cecal  $\gamma\delta$  T cells, germ-free mice were colonized with conventional mouse microbiota for 4 weeks. Although  $\gamma\delta$  T cells produced more IL-17 in germ-free mice than in conventional mice, the transfer of microbiota was sufficient to lower significantly the frequency of cecal IL-17-producing  $\gamma\delta$  T cells, together with a tendency toward a decreased number, and recapitulate the conventional mouse phenotype (Figures 1A and 1B; Figure S1B). In concordance with these results, broad-spectrum antibiotic treatment significantly increased the proportion and absolute number of IL-17<sup>+</sup>  $\gamma\delta$  T cells in the cecum lamina propria (Figures 1C and 1D; Figure S1D) and, more importantly, their production of IL-17 (Figure 1D).

### Vancomycin-sensitive commensals differentially regulate $\gamma\delta$ T cells from various compartments of the gastrointestinal tract

Our data raised the question of whether gut-derived metabolites preferentially found in the cecum could explain this tissue-specific regulation of IL-17-producing  $\gamma\delta$  T cells. To address this question, conventional mice were treated for 3 weeks with either vancomycin, an antibiotic that targets Gram-positive bacteria, including Firmicutes, or colistin, which targets Gram-negative enterobacteria. Our results revealed that colistin failed to

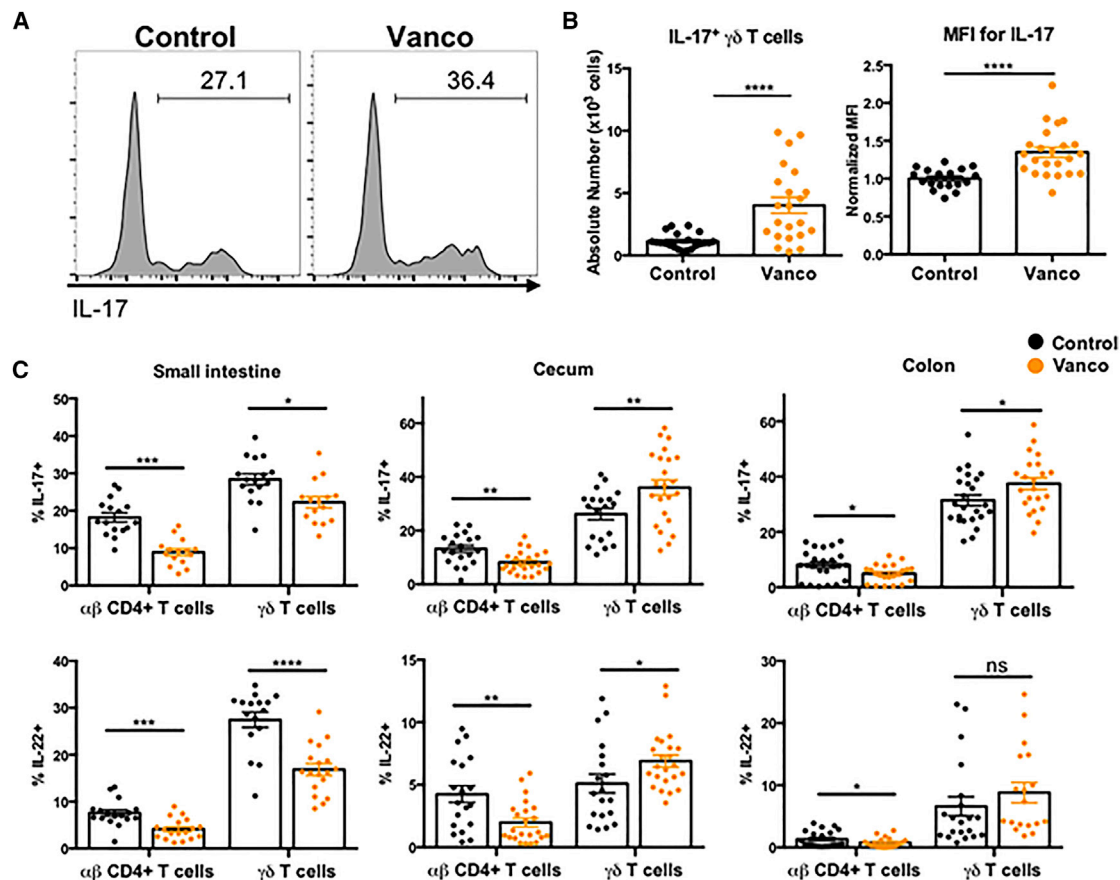


**Figure 2. The gut microbiota regulates differentially IL-17 and IL-22 productions by  $\gamma\delta$  T cells from small intestine, cecum, and colon**  
 (A) Intracellular analysis of IL-17 expression by gated  $\gamma\delta$  T cells from cecum obtained from untreated mice (control) and vancomycin (vanco)-treated mice.  
 (B) Absolute number of IL-17<sup>+</sup>  $\gamma\delta$  T cells (left) and normalized MFI for IL-17 (right) in gated  $\gamma\delta$  T cells obtained as described in (A).  
 (C) Intracellular analysis of IL-17 and IL-22 expression by gated  $\alpha\beta$  CD4<sup>+</sup> T cells and  $\gamma\delta$  T cells from small intestine (left), cecum (middle), and colon (right) obtained from untreated mice (control; black) and vanco-treated mice (orange).  
 In each case, cells were stimulated with PMA + ionomycin + IL-1 $\beta$  + IL-23 for 3 h. Errors bars are SEM from 15 to 24 mice (C) per group. Significant differences were determined using two-tailed Mann-Whitney test: \* $p < 0.05$ ; \*\* $p < 0.01$ ; \*\*\*\* $p < 0.0001$ . See also Figure S2.

modulate IL-17 production by cecal  $\gamma\delta$  T cells (Figures S2A and S2B) but that vancomycin treatment increased IL-17-producing  $\gamma\delta$  T cells in proportion and in absolute number (Figures 2A and 2B). The quantity of IL-17 cytokine produced by cecum  $\gamma\delta$  T cells was also increased, as revealed by median fluorescence intensity (MFI) analysis (Figure 2B). Considering our data for vancomycin, we more deeply analyzed the functional properties of T cells upon administration of this antibiotic. As shown previously by others (Smith et al., 2013; Benakis et al., 2016), conventional Th17 cells were decreased by vancomycin treatment because commensal bacteria are essential to maintain and activate this population in the gut lamina propria of mice (Figure 2C). Concerning  $\gamma\delta$  T cells, we observed a dichotomy according to the compartment analyzed: vancomycin treatment reduced IL-17-producing  $\gamma\delta$  T cells in the small intestine but increased their proportion in the cecum and colon in comparison with untreated mice (Figure 2C). Interestingly, vancomycin treatment also resulted in diminished frequency of IL-22-producing  $\gamma\delta$  T cells in the small intestine and a rise in the cecum and colon. Of note,

the proportion of interferon (IFN)- $\gamma$ -producing  $\gamma\delta$  T cells was not altered in any of the compartments analyzed, suggesting that the microbiota does not impact this specific function (Figure S2C). These data highlight that  $\gamma\delta$  T cells from various compartments of the gastrointestinal tract are differentially regulated by vancomycin-sensitive bacteria. In contrast to the small intestine, the colonic and cecal microbiota repress the activity of IL-17- and IL-22-producing  $\gamma\delta$  T cells.

### SCFAs repress IL-17- and IL-22-producing $\gamma\delta$ T cells

SCFAs are metabolites known for their immunoregulatory properties (Corrêa-Oliveira et al., 2016). Very small amounts are present in the small intestine, as they are mainly synthesized by Firmicutes in the cecum and colon from the fermentation of non-digestible fiber (Cummings et al., 1987). Therefore, SCFAs may explain the repression of IL-17 production by  $\gamma\delta$  T cells in these gut compartments.

As previously reported (Smith et al., 2013), we found that mice treated for 3 weeks with either vancomycin or broad-spectrum



antibiotics exhibited drastic reductions in the concentrations of propionate, butyrate, and acetate, the three most abundant SCFAs in the cecal lumen. Conversely, colistin treatment did not modify SCFA levels (Figure 3A). Furthermore, a strong negative correlation was observed between SCFA abundance and the proportion of IL-17<sup>+</sup> cells or the quantity of IL-17 (MFI) produced by  $\gamma\delta$  T lymphocytes (Figure 3B; Figure S2D). Therefore, we hypothesized that SCFAs may contribute to repressing the production of IL-17 and IL-22 by  $\gamma\delta$  T cells. We first isolated cecal lamina propria cells from conventional mice and incubated them with SCFA in combination (SCFA mix, used in relative proportions representative of physiological conditions in cecum, such as 3:1:1, acetate:butyrate:propionate) (Cummings et al., 1987) or individually (propionate, butyrate, or acetate). Our results revealed that SCFAs inhibited IL-17 production by  $\gamma\delta$  T cells; the proportion of IL-17<sup>+</sup>  $\gamma\delta$  T cells (Figures 3C–3E; Figures S3A and S3B) and the quantity of synthesized IL-17 protein (Figure S3C) were reduced among  $\gamma\delta$  T cells in the presence of SCFAs, with a more drastic effect for propionate. With regard to IL-22, we found reduced production upon propionate exposure (Figures 3D; Figure S3B), especially among IL-17-producing  $\gamma\delta$  T cells (Figures S3A and S3B). It has been previously shown that SCFAs do not significantly alter IL-17-producing  $\alpha\beta$  T cells (Smith et al., 2013). In accordance, we observed that propionate acts specifically on  $\gamma\delta$  T cells without modifying the proportion of conventional Th17 cells (Figure S3D); instead, total production of IL-17 by the whole tissue was increased by propionate (Figure S3E). This result is mainly due to conventional CD4<sup>+</sup>  $\alpha\beta$  T cells, the major producers of IL-17 in the lamina propria.

To evaluate the generality of these observations, we investigated  $\gamma\delta$  T cells from various anatomical sources. The production of IL-17 and IL-22 was inhibited *ex vivo* by propionate with  $\gamma\delta$  T cells isolated from the lamina propria of the small intestine and colon and peripheral organs such as the spleen and lymph nodes (Figure S3F). Thus, SCFAs, especially propionate, repress IL-17- and IL-22-producing  $\gamma\delta$  T cells from distinct organs.

To evaluate whether SCFAs regulate  $\gamma\delta$  T cells *in vivo*, propionate, butyrate, or acetate was added to the drinking water of mice over 3 weeks. However, under these conditions, we did not observe any changes in  $\gamma\delta$  T cell functionalities upon SCFA treatment (Figure S4A), likely because SCFAs are already abundant in the lumen of untreated mice, the system is saturated, and no additional effect can be observed under these conditions (Figure 3A). We then treated mice with vancomycin to disrupt the gut microbiota to decrease SCFA concentrations in the lumen (Figure 3A), allowing analysis of orally supplied metabolites. Under these conditions, vancomycin enhanced IL-17 and IL-22 production by  $\gamma\delta$  T cells, as mentioned above (Figure 2C), and administration of propionate, but not butyrate or acetate, in drinking water over three weeks inhibited  $\gamma\delta$  T cell functionalities (Figures 4A and 4B; Figures S4B–S4D). Thus, propionate is the main metabolite able to inhibit IL-17 production by  $\gamma\delta$  T cells *in vitro* and *in vivo*. It has been previously shown that propionate ameliorates DSS-induced colitis (Tong et al., 2016). Moreover, in this model, immune cells from the lamina propria increased their production of IL-17, and this cytokine and weight loss concomitantly reached a peak at day 9 (Nunes et al., 2019; Lamas et al., 2016). Therefore, we chose this time point to investigate the bio-

logical relevance of propionate relative to IL-17<sup>+</sup>  $\gamma\delta$  T cells. Our data showed a significant reduction in IL-17 and IL-22 production by  $\gamma\delta$  T cells in propionate-treated mice (Figures 4C and 4D), although weight loss was not altered at this time (Figure 4E).

### Propionate reduces IL-17 production by $\gamma\delta$ T cells by inhibiting HDAC

As ROR- $\gamma$ t is required to stimulate IL-17 production, expression of this transcription factor was assessed after SCFA treatment *in vitro*. Approximately 60% of  $\gamma\delta$  T cells in the cecal lamina propria were ROR- $\gamma$ t<sup>+</sup>, and this expression was maintained in the presence of propionate, butyrate, and acetate (Figures S5A–S5C). Therefore, propionate acts on IL-17 production by intestinal  $\gamma\delta$  T cells independently of ROR- $\gamma$ t inhibition, probably because these lymphocytes are already differentiated when they reach the gastrointestinal tract. This is in accordance with conventional T cells, in which ROR- $\gamma$ t expression is decreased by SCFAs during Th17 differentiation, but not in fully differentiated Th17 cells (Salkowska et al., 2017).

As reported previously (Zhang et al., 2016; Nastasi et al., 2017), SCFAs inhibited IL-1 $\beta$  and IL-23 production in the cecum (Figure S5D), suggesting a possible indirect effect of metabolites on  $\gamma\delta$  T cells via macrophages and dendritic cells. Nevertheless, propionate and butyrate inhibited IL-17 production by  $\gamma\delta$  T cells in the absence of IL-1 $\beta$  and IL-23 (Figure S5E). As SCFAs are known to increase the frequency of IL-10-producing regulatory T (Treg) cells (Smith et al., 2013), we then assessed the effect of IL-10 on IL-17 production by  $\gamma\delta$  T cells. Our results revealed that recombinant IL-10 did not inhibit IL-17 production *in vitro* (Figure S5F). Moreover, in the absence of IL-10, propionate maintained its effect on IL-17-producing  $\gamma\delta$  T cells (Figure 5A). Sorted  $\gamma\delta$  T cells were examined to assess the direct effect of SCFAs. Upon stimulation, this cell population produced IL-17, but propionate reduced the proportion of IL-17-competent cells (Figure 5B; Figure S5G). Thus, propionate effectively inhibits  $\gamma\delta$  T cell functions through direct effects. Moreover, these results were not attributable to any toxicity of the metabolite. By contrast, propionate-treated  $\gamma\delta$  T cells upregulated expression of the Bcl2 gene, an anti-apoptotic molecule, in comparison with the control (Figures S5H and S5I). We next investigated the capacity of propionate to modulate the proliferation of  $\gamma\delta$  T cells. In the steady state, this population, namely, CD27<sup>neg</sup>, is a minor subset in comparison with CD27<sup>+</sup> IFN- $\gamma$ -producing  $\gamma\delta$  T cells. IL-7 was used to promote expansion of IL-17-producing  $\gamma\delta$  T cells (Michel et al., 2012), which reached ~70% of the total  $\gamma\delta$  T cells after 5 days of culture. Interestingly, propionate reduced this proliferation, as revealed by the decreased frequency of CD27<sup>neg</sup> (Figure S5J) and the proportion of Ki67<sup>+</sup> cells (population in cycle) (Figure S5K). Of note, this effect was specific to IL-17-producing  $\gamma\delta$  T cells because the frequency of Ki67<sup>+</sup> cells among other populations increased upon propionate treatment (Figure S5K).

Propionate has been shown to mediate some of its beneficial effects via G-protein-coupled receptor (GPR) 41 and GPR43 (Trompette et al., 2014; Maslowski et al., 2009). GPR41 was not detected in  $\gamma\delta$  T cells, while GPR43 was expressed weakly (Figure 5C). Nonetheless, propionate retained its ability to inhibit IL-17 production by  $\gamma\delta$  T cells in GPR43 KO mice (ffar2<sup>-/-</sup>) (Figure 5D). Moreover, the GPR43 antagonist GLPG

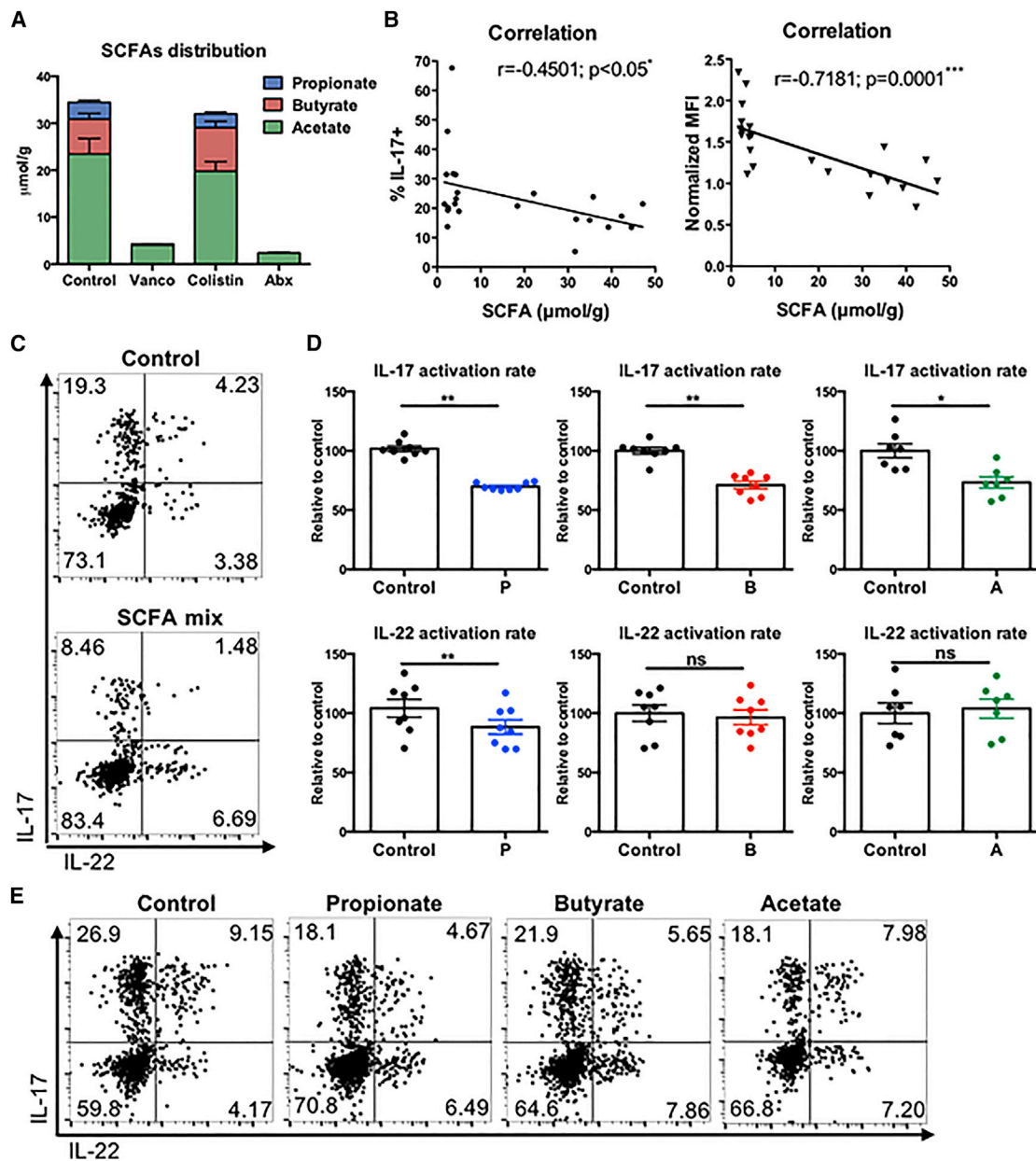


**Figure 3. SCFAs inhibit *ex vivo* IL-17 and IL-22 productions by  $\gamma\delta$  T cells**

(A) Concentrations of propionate (blue), butyrate (red), and acetate (green) per gram of cecal content obtained from untreated mice (control) and mice treated 3 weeks with antibiotics (vanco, colistin, or 4 Abx).

(B) Spearman correlation between SCFAs and IL-17 production (percentage, left or MFI, right) in gated  $\gamma\delta$  T cells from cecum obtained as described in (A).

(C) Total cecal cells were cultured for 4 h with a mix of propionate, butyrate, and acetate (SCFA mix) or PBS (control); activated with PMA + ionomycin + IL-1 $\beta$  + IL-23 for the last 3 h; and stained for intracellular IL-17 and IL-22. Representative plots on gated  $\gamma\delta$  T cells. For all plots, numbers indicate percentage of cells in relevant quadrant.

(D) Total cecal cells were cultured for 4 h with PBS (control), or propionate, butyrate, or acetate activated as described in (C); and stained for intracellular IL-17 and IL-22. A, acetate; B, butyrate; P, propionate.

(E) Representative plots of  $\gamma\delta$  T cells from cecum obtained as described in (D). For all plots, numbers indicate percentage of cells in relevant quadrant.

Errors bars are SEM from 5 to 7 mice per group (A), 23 mice (B), and from 7 to 9 mice (C and D) per group. Significant differences were determined using Wilcoxon test (D): \* $p < 0.05$ ; \*\* $p < 0.01$ . See also Figure S3.

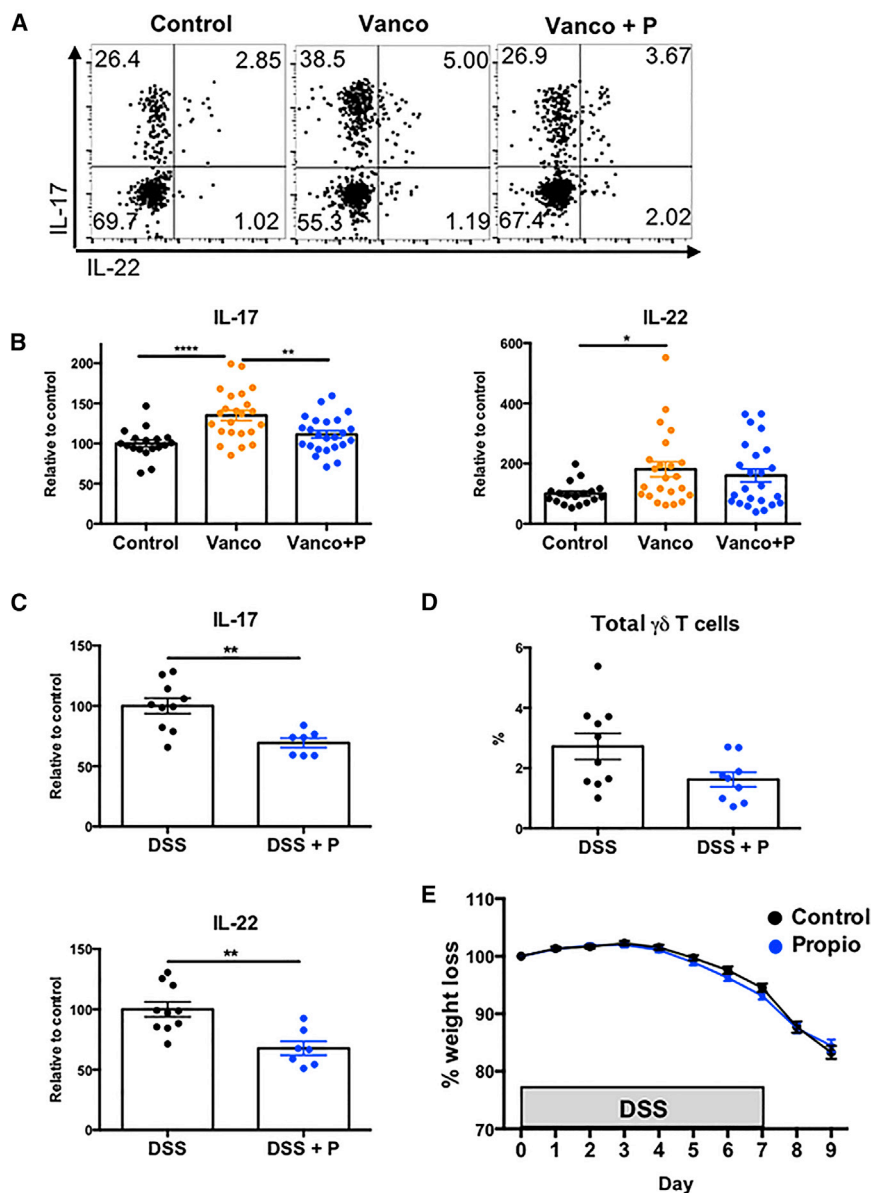


**Figure 4. SCFAs inhibit *in vivo* IL-17 production by  $\gamma\delta$  T cells**

(A) Representative plots of gated  $\gamma\delta$  T cells from cecum from mice treated with PBS (control; black), vanco, or vanco + propionate. For all plots, numbers indicate percentage of cells in relevant quadrant. P, propionate.

(B) Percentage of IL-17<sup>+</sup> and IL-22<sup>+</sup>  $\gamma\delta$  T cells from mice treated as described in (A). P, propionate.

(C and D) DSS-exposed mice were treated with PBS (control; black) or propionate (blue). Total percentage of  $\gamma\delta$  T cells and production of IL-17 and IL-22 by cecal  $\gamma\delta$  T cells on day 9 after initiation of DSS treatment. P, propionate.

(E) Weight loss of DSS-exposed mice were treated with PBS (control; black) or propionate (blue). Data are mean  $\pm$  SEM of five experiments. Propio, propionate.

In each case, cells were stimulated with PMA + ionomycin + IL-1 $\beta$  + IL-23 for 3 h. Error bars are SEM from 17 to 24 mice per group (A) and from 9 to 10 mice (C–E) per group. Significant differences were determined using ordinary one-way ANOVA (B) and two-tailed Mann-Whitney test (C and D): \* $p < 0.05$ ; \*\* $p < 0.01$ ; \*\*\*\* $p < 0.0001$ . See also Figure S4.

When cecal immune cells were incubated with trichostatin A (TSA), a well-known HDAC inhibitor, IL-17 production was reduced, mimicking the effect of propionate (Figure 5F). Interestingly, coincubation of propionate and TSA did not have any additive effect in comparison to propionate or TSA alone, which suggests that HDAC inhibition is a mechanism by which propionate acts on  $\gamma\delta$  T cell functionalities.

### Propionate represses IL-17 production by human $\gamma\delta$ T cells from patients with IBD

In contrast to mice, human IL-17-producing  $\gamma\delta$  T lymphocytes are rarely detected

0974 failed to block the effect of propionate on  $\gamma\delta$  T cells (Figure 5E). Another possibility is that SCFAs may enter via a transporter (Singh et al., 2010) and directly act as inhibitors of HDAC, an enzyme that regulates gene expression, activity (Biolotta and Cong, 2019). MCT1 (monocarboxylate transporter-1) and SMCT1 (sodium-coupled monocarboxylate transporter-1) are the major proteins involved in the transport of SCFAs (Sivaprakasam et al., 2017), and  $\gamma\delta$  T cells preferentially express MCT1 (Figure 5C). To evaluate whether MCT1 plays a role in the transport of propionate into  $\gamma\delta$  T lymphocytes, cecal cells were pretreated with an MCT1/2 inhibitor (AR-C155858) before stimulation with propionate. Blocking MCT1/2 did not alter the effect of propionate on IL-17 production by  $\gamma\delta$  T cells, suggesting that propionate is not actively transported by MCT1 (Figure 5E).

in healthy adults (Michel et al., 2012). However, we observed that a significant proportion of patients with IBD (~40%) display a small population of peripheral  $\gamma\delta$  T cells that can produce IL-17 (Figures S6A and S6B). Among IL-17 producers, treatment with propionate or a mixture of SCFAs induced a 3-fold reduction in IL-17-positive cells (Figures 6A and 6B). Conversely, no effect was observed regarding IL-22 and IFN- $\gamma$  (Figure S6C). Hence, as in mice, SCFAs inhibit the production of IL-17 by  $\gamma\delta$  T cells in humans.

Furthermore, a mixture of SCFAs was also able to slightly repress IL-17 production by another innate T population called MAIT (mucosal associated-invariant T) cells (Figure S6D) from humans, although interestingly, this inhibition was not significant with propionate alone. Consistent with the specific effect of propionate on IL-17-producing  $\gamma\delta$  T cells, IL-17 inhibition by the



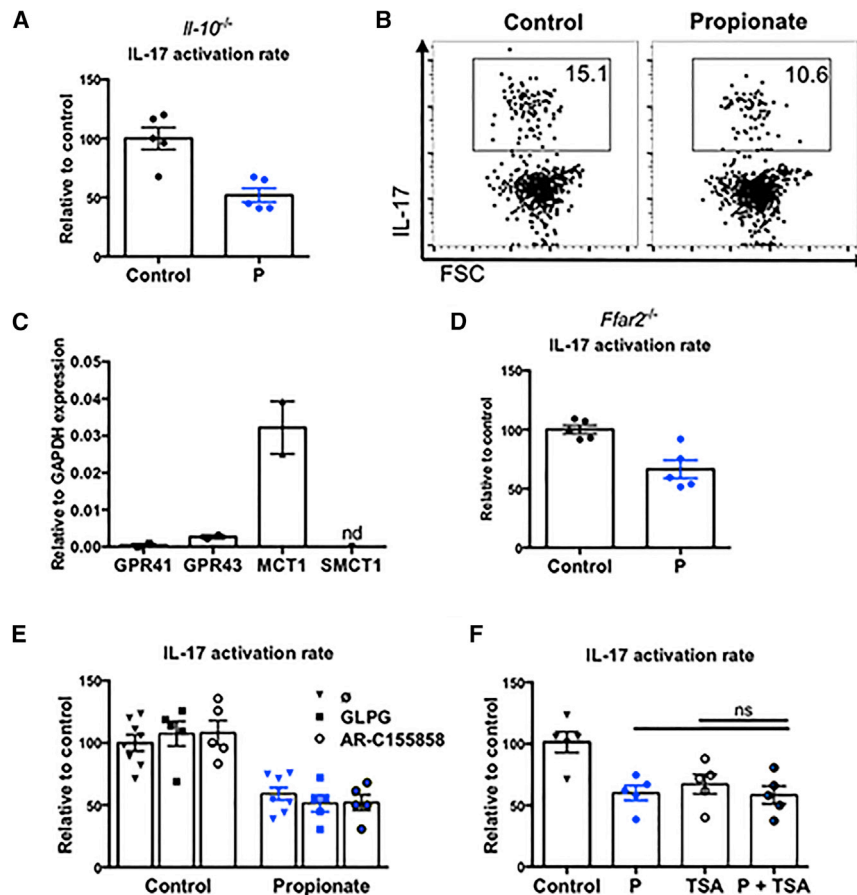


**Figure 5. HDACs mediate propionate effects on  $\gamma\delta$  T cells**

(A) IL-17 production by cecal  $\gamma\delta$  T cells obtained from *Il10*<sup>-/-</sup> mice treated 4 h with PBS (control) or propionate, and stimulated with PMA + ionomycin + IL-1 $\beta$  + IL-23 for the last 3 h. Error bars are SEM from n = 5 mice. P, propionate.

(B) Sorted  $\gamma\delta$  T cells from peripheral lymph nodes were cultured for 18 h with PBS (control) or propionate and stimulated as described in (A). Representative plots on gated  $\gamma\delta$  T cells (n = 4). For all plots, number indicates percentage of IL-17<sup>+</sup> cells.

(C) GPR41, GPR43, MCT1, and SMCT1 mRNA quantification by qPCR in sorted  $\gamma\delta$  T cells from peripheral lymph nodes. Error bars are SEM from n = 2. nd, not detected.

(D) IL-17 production by cecal  $\gamma\delta$  T cells obtained from *Ffar2*<sup>-/-</sup> mice treated 4 h with PBS (control) or propionate and stimulated as described in (A). Error bars are SEM from n = 5 mice. P, propionate. (E and F) IL-17 activation rate relative to control on gated  $\gamma\delta$  T cells from cecum cultured for 4 h with propionate and/or GLPG 0974, AR-C155858 (E), or TSA (F) and stimulated as described in (A). Error bars are SEM from n = 5 mice. Significant differences were determined using Wilcoxon test. P, propionate.

See also [Figures S5 and S6](#).

occurs through GPR43, it does not mediate the effect of propionate on IL-17 production by  $\gamma\delta$  T cells but may affect other downstream targets through this receptor. Despite expression of GPR43

HDAC inhibitor was observed only in  $\gamma\delta$  T cells and not in MAIT cells ([Figure 6C](#); [Figure S6E](#)).

## DISCUSSION

In this study, we provide insight into the mechanisms of regulation of intestinal IL-17-producing  $\gamma\delta$  T cells in mice and humans. IL-17-producing  $\gamma\delta$  T cells are repressed by SCFAs in the cecum and colon, and antibiotic treatment eliminates this inhibition without affecting IFN- $\gamma$ -producing cells. Thus, manipulating the concentration of SCFAs *in vivo* may regulate the balance between IL-17- and IFN- $\gamma$ -producing  $\gamma\delta$  T cells. Future experiments to evaluate the effect of SCFAs on other innate T cells, such as MAIT and iNKT (invariant natural killer T) cells, are warranted.

As innate lymphoid 3 cells (ILC3s) ([Sawa et al., 2011](#)), cecal  $\gamma\delta$  T lymphocytes do not need microbiota to produce IL-17 and IL-22; they are programmed in the thymus. However, microbiota-derived metabolites differentially regulate ILC3s and  $\gamma\delta$  T cells. While propionate acts directly on intestinal  $\gamma\delta$  T cells to inhibit IL-17 and IL-22 production, this SCFA increases the proportion of IL-22<sup>+</sup> ILC3s but does not alter IL-17 production by this population ([Chun et al., 2019](#)). These results suggest that the mechanisms of action of SCFAs on ILC3s and  $\gamma\delta$  T cells may be distinct. Indeed, although the regulation of colonic ILC3 function

on intestinal macrophages, butyrate does not act via this receptor but regulates macrophage function via HDAC inhibition ([Chang et al., 2014](#)).

The same appears to be true for the  $\gamma\delta$  T cells with IL-17 production that is dependent on HDAC activity. TSA is a potent inhibitor of classes I (HDACs 1, 2, 3, and 8), IIa (HDACs 4, 5, 7, and 9), and IIb (HDACs 6 and 10) HDACs. Several HDACs have already been associated with IL-17 regulation, such as HDAC1, HDAC3, and HDAC6. In addition, specific inhibition of HDAC6 in  $\gamma\delta$  T cells was reported to promote IL-17 expression ([Yan et al., 2017](#)). Conversely, both HDAC1 and HDAC3 appear to exert positive effects on IL-17 production, as HDAC3 is required for IL-17 production by iNKT cells ([Thapa et al., 2017](#)) and HDAC1 can interact with ROR- $\gamma$ t, reduce its acetylation level, and then enhance transcriptional activation of IL-17 ([Wu et al., 2015](#)). Therefore, our data suggest that propionate may affect IL-17 production by  $\gamma\delta$  T cells through HDAC inhibition, possibly involving HDAC1 or HDAC3. As HDAC is an intracellular target, propionate probably enters  $\gamma\delta$  T cells. The transporter MCT1 is expressed by IL-17-producing  $\gamma\delta$  T cells but is not involved in the action of propionate. Therefore, the mechanism of propionate uptake into  $\gamma\delta$  T cells is likely dependent on passive diffusion through the plasma membrane, as observed for macrophages ([Chang et al., 2014](#)).

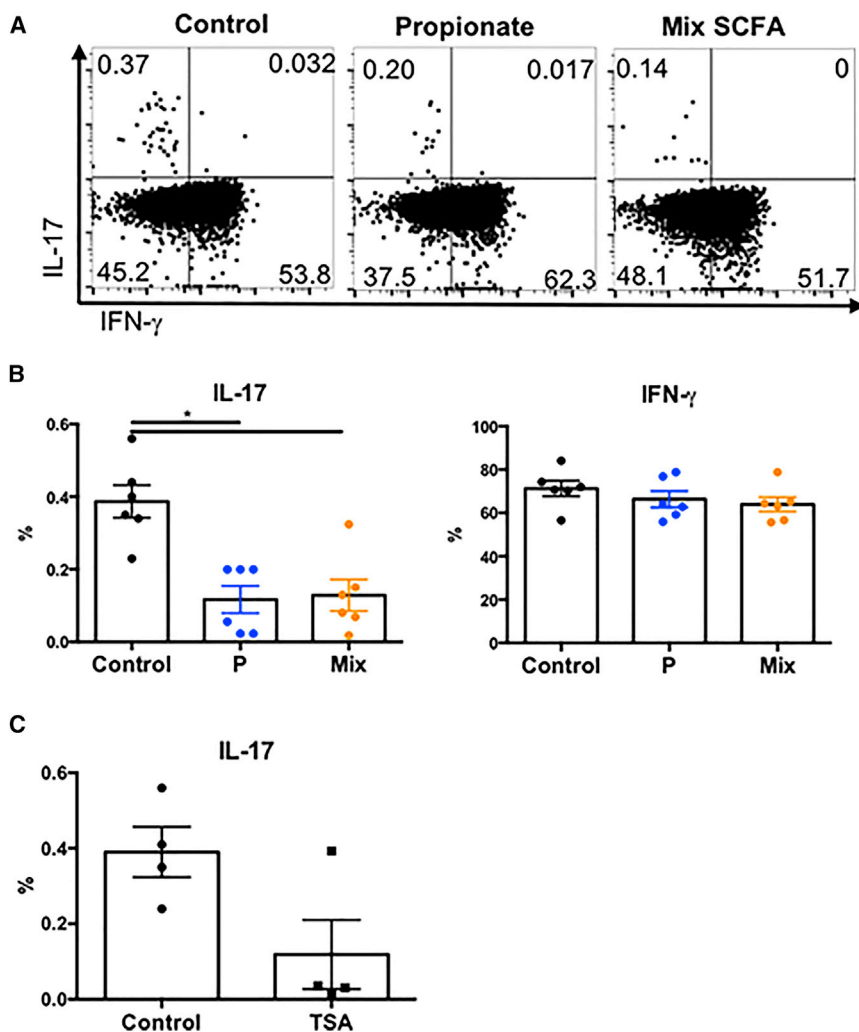


**Figure 6. SCFAs inhibit IL-17 production by human  $\gamma\delta$  T cells**

(A) Intracellular analysis of IL-17 and IFN- $\gamma$  expression by gated  $\gamma\delta$  T cells from peripheral blood mononuclear cells (PBMCs) of patients with IBD, untreated (control), or treated 18 h with propionate or a mix of SCFAs (mix) and stimulated with PMA + ionomycin for the last 5 h. Representative plots from  $n = 6$ . For all plots, numbers indicate percentage of cells in relevant quadrant. (B) Collective analysis of IL-17 and IFN- $\gamma$  expression by gated  $\gamma\delta$  T cells from patients with IBD, treated as described in (A). \* $p < 0.05$  versus control (non-parametric Friedman test). P, propionate. (C) IL-17 activation production by gated  $\gamma\delta$  T cells from patients with IBD, treated 18 h with PBS (control) or TSA and activated as described in (A). Error bars are SEM from  $n = 4$ . See also Figure S7.

Although SCFAs are synthesized in the lumen of the cecum and colon, they are absorbed by epithelial cells and enter into the systemic circulation. High SCFA levels have been associated with attenuated inflammation, such as autoimmune hepatitis (Hu et al., 2018) and allergic airway disease (Trompette et al., 2014), but worsened defense against pathogens, such as *Staphylococcus aureus*, in a pneumonia context (Tian et al., 2019). This suggests pathologic situations in which potential dysregulation of IL-17- and IL-22-producing  $\gamma\delta$  T cells should be examined.

Finally, human IL-17-producing  $\gamma\delta$  T cells appear to be more abundant in the intestinal mucosa of patients with IBD and tumor colorectal tissue (Wu et al., 2014; Presti et al., 2019). Considering their deleterious role, the effect of propionate on human  $\gamma\delta$  T cell activity may provide a pathway of regulation to prevent cancer progression and chronic inflammatory processes. More widely, SCFA levels have been found to be reduced in the feces of patients with IBD (Lavelle and Sokol, 2020). However, their role in colitis is ambiguous, as their beneficial effect on inflammation can be partially counteracted by a delay in tissue repair (Kaiko

et al., 2016). Future applications of our data will permit us to better understand the dual role of microbiota-derived metabolites in IBD.

## STAR★METHODS

Detailed methods are provided in the online version of this paper and include the following:

- KEY RESOURCES TABLE
- RESOURCE AVAILABILITY
  - Lead contact
  - Materials availability
  - Data and code availability
- EXPERIMENTAL MODEL AND SUBJECT DETAILS
  - Mouse models
  - Human subjects
- METHOD DETAILS
  - Antibiotic and SCFA treatment
  - DSS-induced colitis model
  - Germ-free (GF) experiment

- Cell preparation
- Human PBMCs isolation
- *In vitro* culture assays
- Flow cytometry and cell sorting
- SCFA analysis in cecal samples
- RNA expression analysis
- Cytokine quantification

● **QUANTIFICATION AND STATISTICAL ANALYSIS**

**SUPPLEMENTAL INFORMATION**

Supplemental information can be found online at <https://doi.org/10.1016/j.celrep.2021.109332>.

**ACKNOWLEDGMENTS**

We thank the team “Vaccines, Virus and Immunopathologies” (Molecular Immunology and Virology unit, INRA) and the Animal Facilities (ANAXEM germ-free platform and IERP, INRAE) staff for support. We thank Marie-Anne Nahori for assistance and N. Lapaque for discussions and reagents. L.D. is supported by the Foundation for Medical Research. This work is supported, in part, by the Association Francois Aupetit.

**AUTHOR CONTRIBUTIONS**

L.D., H.S., and M.-L.M. designed the study and analyzed and interpreted the data. A.M., N.R., M.L.R., G.D.C., S.T., C. Mayeur, J.P., A.A., C.D., C. Michaudel, and M.S. provided technical help. F.T. provided *ffar2*<sup>-/-</sup> mice. L.D., A.M., N.R., F.T., P.L., H.S., and M.-L.M. discussed the experiments and results. L.D., H.S., and M.-L.M. wrote the manuscript. All authors read and approved the final manuscript.

**DECLARATION OF INTERESTS**

The authors declare no competing interests.

Received: August 12, 2020

Revised: March 4, 2021

Accepted: June 10, 2021

Published: July 6, 2021

**SUPPORTING CITATIONS**

The following references appear in the supplemental information: Cha et al. (2010); Conway et al. (2012); Fachi et al. (2020); Li et al. (2014); Tomkovich et al. (2017).

**REFERENCES**

Benakis, C., Brea, D., Caballero, S., Faraco, G., Moore, J., Murphy, M., Sita, G., Racchumi, G., Ling, L., Pamer, E.G., et al. (2016). Commensal microbiota affects ischemic stroke outcome by regulating intestinal  $\gamma\delta$  T cells. *Nat. Med.* **22**, 516–523.

Bilotta, A.J., and Cong, Y. (2019). Gut microbiota metabolite regulation of host defenses at mucosal surfaces: implication in precision medicine. *Precis. Clin. Med.* **2**, 110–119.

Cha, H.-R., Chang, S.-Y., Chang, J.-H., Kim, J.-O., Yang, J.-Y., Kim, C.-H., and Kweon, M.-N. (2010). Downregulation of Th17 Cells in the Small Intestine by Disruption of Gut Flora in the Absence of Retinoic Acid. *J. Immunol.* **184**, 6799–6806.

Chang, P.V., Hao, L., Offermanns, S., and Medzhitov, R. (2014). The microbial metabolite butyrate regulates intestinal macrophage function via histone deacetylase inhibition. *Proc. Natl. Acad. Sci. USA* **111**, 2247–2252.

Chen, Y.-S., Chen, I.-B., Pham, G., Shao, T.-Y., Bangar, H., Way, S.S., and Haslam, D.B. (2020). IL-17-producing  $\gamma\delta$  T cells protect against *Clostridium difficile* infection. *J. Clin. Invest.* **130**, 2377–2390.

Cheng, M., Qian, L., Shen, G., Bian, G., Xu, T., Xu, W., Shen, G., and Hu, S. (2014). Microbiota modulate tumoral immune surveillance in lung through a  $\gamma\delta$ T17 immune cell-dependent mechanism. *Cancer Res.* **74**, 4030–4041.

Chien, Y.-H., Meyer, C., and Bonneville, M. (2014).  $\gamma\delta$  T Cells: First Line of Defense and Beyond. *Annu. Rev. Immunol.* **32**, 121–155.

Chun, E., Lavoie, S., Fonseca-Pereira, D., Bae, S., Michaud, M., Hoveyda, H.R., Fraser, G.L., Gallini Comeau, C.A., Glickman, J.N., Fuller, M.H., et al. (2019). Metabolite-Sensing Receptor Ffar2 Regulates Colonic Group 3 Innate Lymphoid Cells and Gut Immunity. *Immunity* **51**, 871–884.e6.

Conway, K.L., Goel, G., Sokol, H., Manocha, M., Mizoguchi, E., Terhorst, C., Bhan, A.K., Gardet, A., and Xavier, R.J. (2012). p40phox Expression Regulates Neutrophil Recruitment and Function During the Resolution Phase of Intestinal Inflammation. *J. Immunol.* **189**, 3631–3640.

Corrêa-Oliveira, R., Fachi, J.L., Vieira, A., Sato, F.T., and Vinolo, M.A. (2016). Regulation of immune cell function by short-chain fatty acids. *Clin. Transl. Immunol.* **5**, e73.

Cummings, J.H., Pomare, E.W., Branch, W.J., Naylor, C.P., and Macfarlane, G.T. (1987). Short chain fatty acids in human large intestine, portal, hepatic and venous blood. *Gut* **28**, 1221–1227.

Do, J.S., Visperas, A., Dong, C., Baldwin, W.M., 3rd, and Min, B. (2011). Cutting edge: Generation of colitogenic Th17 CD4 T cells is enhanced by IL-17+  $\gamma\delta$  T cells. *J. Immunol.* **186**, 4546–4550.

D’Ombra, M.C., Hansen, D.S., Simpson, K.M., and Schofield, L. (2007).  $\gamma\delta$  T cells expressing NK receptors predominate over NK cells and conventional T cells in the innate IFN- $\gamma$  response to Plasmodium falciparum malaria. *Eur. J. Immunol.* **37**, 1864–1873.

Duan, J., Chung, H., Troy, E., and Kasper, D.L. (2010). Microbial colonization drives expansion of IL-1 receptor 1-expressing and IL-17-producing  $\gamma\delta$  T cells. *Cell Host Microbe* **7**, 140–150.

Fachi, J.L., Sécça, C., Rodrigues, P.B., Mato, F.C.P., Di Luccia, B., Felipe, J.S., Pral, L.P., Rungue, M., Rocha, V.M., Sato, F.T., et al. (2020). Acetate coordinates neutrophil and ILC3 responses against *C. difficile* through FFAR2. *J. Exp. Med.* **217**, e20190489.

Geddes, K., Rubino, S.J., Magalhaes, J.G., Streutker, C., Le Bourhis, L., Cho, J.H., Robertson, S.J., Kim, C.J., Kaul, R., Philpott, D.J., and Girardin, S.E. (2011). Identification of an innate T helper type 17 response to intestinal bacterial pathogens. *Nat. Med.* **17**, 837–844.

Hu, E.-D., Chen, D.-Z., Wu, J.-L., Lu, F.-B., Chen, L., Zheng, M.-H., Li, H., Huang, Y., Li, J., Jin, X.Y., et al. (2018). High fiber dietary and sodium butyrate attenuate experimental autoimmune hepatitis through regulation of immune regulatory cells and intestinal barrier. *Cell. Immunol.* **328**, 24–32.

Hueber, W., Sands, B.E., Lewitzky, S., Vandemeulebroecke, M., Reinisch, W., Higgins, P.D.R., Wehkamp, J., Feagan, B.G., Yao, M.D., Karczewski, M., et al. (2012). Secukinumab, a human anti-IL-17A monoclonal antibody, for moderate to severe Crohn’s disease: unexpected results of a randomised, double-blind placebo-controlled trial. *Gut* **61**, 1693–1700.

Kaiko, G.E., Ryu, S.H., Koues, O.I., Collins, P.L., Solnica-Krezel, L., Pearce, E.J., Pearce, E.L., Oltz, E.M., and Stappenbeck, T.S. (2016). The Colonic Crypt Protects Stem Cells from Microbiota-Derived Metabolites. *Cell* **165**, 1708–1720.

Kühl, A.A., Pawlowski, N.N., Grollrich, K., Loddenkemper, C., Zeitz, M., and Hoffmann, J.C. (2007). Aggravation of intestinal inflammation by depletion/deficiency of  $\gamma\delta$  T cells in different types of IBD animal models. *J. Leukoc. Biol.* **81**, 168–175.

Lamas, B., Richard, M.L., Leducq, V., Pham, H.-P., Michel, M.-L., Da Costa, G., Bridonneau, C., Jegou, S., Hoffmann, T.W., Natividad, J.M., et al. (2016). CARD9 impacts colitis by altering gut microbiota metabolism of tryptophan into aryl hydrocarbon receptor ligands. *Nat. Med.* **22**, 598–605.

- Lavelle, A., and Sokol, H. (2020). Gut microbiota-derived metabolites as key actors in inflammatory bowel disease. *Nat. Rev. Gastroenterol. Hepatol.* *17*, 223–237.
- Li, Y., Innocentin, S., Withers, D.R., Roberts, N.A., Gallagher, A.R., Grigorieva, E.F., Wilhelm, C., and Veldhoen, M. (2011). Exogenous stimuli maintain intraepithelial lymphocytes via aryl hydrocarbon receptor activation. *Cell* *147*, 629–640.
- Li, J., Chen, S., Qiang, J., Wang, X., Chen, L., and Zou, D. (2014). Diet-induced obesity mediates a proinflammatory response in pancreatic  $\beta$  cell via toll-like receptor 4. *Cent. Eur. J. Immunol.* *39*, 306–315.
- Li, F., Hao, X., Chen, Y., Bai, L., Gao, X., Lian, Z., Wei, H., Sun, R., and Tian, Z. (2017). The microbiota maintain homeostasis of liver-resident  $\gamma\delta$ T-17 cells in a lipid antigen/CD1d-dependent manner. *Nat. Commun.* *7*, 13839.
- Maslowski, K.M., Vieira, A.T., Ng, A., Kranich, J., Sierro, F., Yu, D., Schilter, H.C., Rolph, M.S., Mackay, F., Artis, D., et al. (2009). Regulation of inflammatory responses by gut microbiota and chemoattractant receptor GPR43. *Nature* *461*, 1282–1286.
- McCarthy, N.E., Bashir, Z., Vossenkamper, A., Hedin, C.R., Giles, E.M., Bhattacharjee, S., Brown, S.G., et al. (2013). Proinflammatory V2+ T Cells Populate the Human Intestinal Mucosa and Enhance IFN- Production by Colonic T Cells. *J. Immunol.* *191*, 2752–2763.
- Michel, M.-L., Pang, D.J., Haque, S.F.Y., Potocnik, A.J., Pennington, D.J., and Hayday, A.C. (2012). Interleukin 7 (IL-7) selectively promotes mouse and human IL-17-producing  $\gamma\delta$  cells. *Proc. Natl. Acad. Sci. USA* *109*, 17549–17554.
- Nastasi, C., Fredholm, S., Willerslev-Olsen, A., Hansen, M., Bonefeld, C.M., Geisler, C., Andersen, M.H., Ødum, N., and Woetmann, A. (2017). Butyrate and propionate inhibit antigen-specific CD8<sup>+</sup> T cell activation by suppressing IL-12 production by antigen-presenting cells. *Sci. Rep.* *7*, 14516.
- Nunes, N.S., Chandran, P., Sundby, M., Visioli, F., da Costa Gonçalves, F., Burks, S.R., Paz, A.H., and Frank, J.A. (2019). Therapeutic ultrasound attenuates DSS-induced colitis through the cholinergic anti-inflammatory pathway. *EBioMedicine* *45*, 495–510.
- Presti, E.L., Di Mitri, R., Mocciano, F., Di Stefano, A.B., Scibetta, N., Cicero, G., Pecoraro, G., Conte, E., Dieli, F., and Meraviglia, S. (2019). Characterization of  $\gamma\delta$  T Cells in Intestinal Mucosa from Patients with Early Onset or Long Standing Inflammatory Bowel Disease and Their Correlation with Clinical Status. *J. Crohns Colitis* *13*, 873–883.
- Sałkowska, A., Karaś, K., Walczak-Drzewiecka, A., Dastyk, J., and Ratajewski, M. (2017). Differentiation stage-specific effect of histone deacetylase inhibitors on the expression of ROR $\gamma$ T in human lymphocytes. *J. Leukoc. Biol.* *102*, 1487–1495.
- Sawa, S., Lochner, M., Satoh-Takayama, N., Dulauroy, S., Bérard, M., Kleinschek, M., Cua, D., Di Santo, J.P., and Eberl, G. (2011). ROR $\gamma$ t<sup>+</sup> innate lymphoid cells regulate intestinal homeostasis by integrating negative signals from the symbiotic microbiota. *Nat. Immunol.* *12*, 320–326.
- Sheridan, B.S., Romagnoli, P.A., Pham, Q.-M., Fu, H.-H., Alonzo, F., 3rd, Schubert, W.-D., Freitag, N.E., and Lefrançois, L. (2013).  $\gamma\delta$  T cells exhibit multifunctional and protective memory in intestinal tissues. *Immunity* *39*, 184–195.
- Silva-Santos, B., Serre, K., and Norell, H. (2015).  $\gamma\delta$  T cells in cancer. *Nat. Rev. Immunol.* *15*, 683–691.
- Singh, N., Thangaraju, M., Prasad, P.D., Martin, P.M., Lambert, N.A., Boettger, T., Offermanns, S., and Ganapathy, V. (2010). Blockade of dendritic cell development by bacterial fermentation products butyrate and propionate through a transporter (Slc5a8)-dependent inhibition of histone deacetylases. *J. Biol. Chem.* *285*, 27601–27608.
- Sivaprakasam, S., Bhutia, Y.D., Yang, S., and Ganapathy, V. (2017). Short-Chain Fatty Acid Transporters: Role in Colonic Homeostasis. *Compr. Physiol.* *8*, 299–314.
- Smith, P.M., Howitt, M.R., Panikov, N., Michaud, M., Gallini, C.A., Bohlooly-Y, M., Glickman, J.N., and Garrett, W.S. (2013). The microbial metabolites, short-chain fatty acids, regulate colonic Treg cell homeostasis. *Science* *341*, 569–573.
- Thapa, P., Romero Arocha, S., Chung, J.Y., Sant'Angelo, D.B., and Shapiro, V.S. (2017). Histone deacetylase 3 is required for iNKT cell development. *Sci. Rep.* *7*, 5784.
- Thursby, E., and Juge, N. (2017). Introduction to the human gut microbiota. *Biochem. J.* *474*, 1823–1836.
- Tian, X., Hellman, J., Horswill, A.R., Crosby, H.A., Francis, K.P., and Prakash, A. (2019). Elevated Gut Microbiome-Derived Propionate Levels Are Associated With Reduced Sterile Lung Inflammation and Bacterial Immunity in Mice. *Front. Microbiol.* *10*, 159.
- Tomkovich, S., Yang, Y., Winglee, K., Gauthier, J., Mühlbauer, M., Sun, X., Mohamadzadeh, M., Liu, X., Martin, P., Wang, G.P., et al. (2017). Locoregional Effects of Microbiota in a Preclinical Model of Colon Carcinogenesis. *Cancer Res.* *77*, 2620–2632.
- Tong, L.-C., Wang, Y., Wang, Z.-B., Liu, W.-Y., Sun, S., Li, L., Su, D.-F., and Zhang, L.-C. (2016). Propionate Ameliorates Dextran Sodium Sulfate-Induced Colitis by Improving Intestinal Barrier Function and Reducing Inflammation and Oxidative Stress. *Front. Pharmacol.* *7*, 253.
- Trompette, A., Gollwitzer, E.S., Yadava, K., Sichelstiel, A.K., Sprenger, N., Ngom-Bru, C., Blanchard, C., Junt, T., Nicod, L.P., Harris, N.L., and Marsland, B.J. (2014). Gut microbiota metabolism of dietary fiber influences allergic airway disease and hematopoiesis. *Nat. Med.* *20*, 159–166.
- Workalemahu, G., Foerster, M., Kroegel, C., and Braun, R.K. (2003). Human gamma  $\delta$ -T lymphocytes express and synthesize connective tissue growth factor: effect of IL-15 and TGF- $\beta$  1 and comparison with alpha  $\beta$ -T lymphocytes. *J. Immunol.* *170*, 153–157.
- Wu, P., Wu, D., Ni, C., Ye, J., Chen, W., Hu, G., Wang, Z., Wang, C., Zhang, Z., Xia, W., et al. (2014).  $\gamma\delta$ T17 cells promote the accumulation and expansion of myeloid-derived suppressor cells in human colorectal cancer. *Immunity* *40*, 785–800.
- Wu, Q., Nie, J., Gao, Y., Xu, P., Sun, Q., Yang, J., Han, L., Chen, Z., Wang, X., Lv, L., et al. (2015). Reciprocal regulation of ROR $\gamma$ t acetylation and function by p300 and HDAC1. *Sci. Rep.* *5*, 16355.
- Yan, B., Liu, Y., Bai, H., Chen, M., Xie, S., Li, D., Liu, M., and Zhou, J. (2017). HDAC6 regulates IL-17 expression in T lymphocytes: implications for HDAC6-targeted therapies. *Theranostics* *7*, 1002–1009.
- Zhang, M., Zhou, Q., Dorfman, R.G., Huang, X., Fan, T., Zhang, H., Zhang, J., and Yu, C. (2016). Butyrate inhibits interleukin-17 and generates Tregs to ameliorate colorectal colitis in rats. *BMC Gastroenterol.* *16*, 84.

STAR★METHODS

KEY RESOURCES TABLE

REAGENT or RESOURCE	SOURCE	IDENTIFIER
<b>Antibodies</b>		
APC-labeled anti-mouse TCR $\gamma\delta$ (GL3)	eBioscience	Cat# 17-5711-82; RRID: AB_842756
FITC-labeled anti-mouse CD3 $\epsilon$ (145-2C11)	eBioscience	Cat# 11-0031-85; RRID: AB_464883
APC-eF780-labeled anti-mouse CD3 (145-2C11)	eBioscience	Cat# 47-0031-82; RRID: AB_11149861
PE-labeled anti-mouse CD4 (RM4-5)	eBioscience	Cat# 12-0042-83; RRID: AB_465511
anti-CD16/32 (93)	eBioscience	Cat# 14-0161-85; RRID: AB_467134
PE/Cy7-labeled anti-mouse IFN- $\gamma$ (XMG1.2)	eBioscience	Cat# 25-7311-82; RRID: AB_469680
eF450-labeled anti-mouse IL-17 (17B7)	eBioscience	Cat# 48-7177-82; RRID: AB_11149503
PerCP-eF710-labeled anti-mouse IL-22 (1H8PWSR)	eBioscience	Cat# 46-7221-82; RRID: AB_10598646
PE-labeled anti-mouse ROR- $\gamma$ T (AFKJS-9)	eBioscience	Cat# 12-6988-82; RRID: AB_1834470
eF450-labeled anti-mouse FOXP3 (FJK-16 s)	eBioscience	Cat# 48-5773-82; RRID: AB_1518812
PE-labeled anti-mouse IL-22 (Poly5164)	BioLegend	Cat# 516404; RRID: AB_2124255
BV785-labeled anti-mouse CD4 (RM4-5)	BioLegend	Cat# 100552; RRID: AB_2563053
BV605-labeled anti-mouse CD8 $\alpha$ (53-6.7)	BioLegend	Cat# 100744; RRID: AB_2562609
BV421-labeled anti-mouse CD27 (LG.3A10)	BioLegend	Cat# 124223; RRID: AB_2565547
BV711-labeled anti-human CD3 $\epsilon$ (UCHT1)	BioLegend	Cat# 300464; RRID: AB_2566036
AF700-labeled anti-human CD4 (RPA-T4)	BioLegend	Cat# 300526; RRID: AB_493743
BV605-labeled anti-human CD8 $\alpha$ (RPA-T8)	BioLegend	Cat# 301040; RRID: AB_2563185
AF647-labeled anti-human TCR $\gamma\delta$ (B1)	BioLegend	Cat# 331214; RRID: AB_1089210
BV785-labeled anti-human CD161 (HP-3G10)	BioLegend	Cat# 339930; RRID: AB_2563968
PB-labeled anti-human IL-17 (BL168)	BioLegend	Cat# 512312; RRID: AB_961392
PE/Cy7-labeled anti-human IL-22 (2G12A41)	BioLegend	Cat# 366708; RRID: AB_2571931
APC/Fire750-labeled anti-human IFN- $\gamma$ (4S.B3)	BioLegend	Cat# 502548; RRID: AB_2572107
PE anti-human TCR V $\alpha$ 7.2 (3C10)	BioLegend	Cat# 351706; RRID: AB_10899577
FITC mouse anti-Ki-67 set	BD PharMingen	Cat# 556026; RRID: AB_396302
<b>Biological samples</b>		
whole blood from patients with IBD	Gastroenterology Department of the Saint Antoine Hospital (APHP, Paris, France)	N/A
<b>Chemicals, peptides, and recombinant proteins</b>		
Sodium propionate	Sigma-Aldrich	Cat# P5436-100G
Sodium acetate	Sigma-Aldrich	Cat# S5636-250G
Sodium butyrate	Sigma-Aldrich	Cat# 303410-100G
Sucrose	Sigma-Aldrich	Cat# S7903-1KG
Vancomycin (chlorhydrate)	Mylan	Cat# 1g
Colistin sulfate salt	Sigma-Aldrich	Cat# C4461-1G
Ampicillin	Euromedex	Cat# UA2262-A
Neomycin sulfate	Euromedex	Cat# UN1015-B
Metronidazole	Toku-e	Cat# M011-25G
DSS / Dextran sulfate sodium salt, colitis grade (36,000 - 50,000)	MP Biomedicals	Cat# 0216011080
Bacto Brain Heart Infusion	BD	Cat# 237500
Bacto Yeast Extract	BD	Cat# 212750
Hemine from bovine	Sigma-Aldrich	Cat# H9039
Cysteine	Sigma-Aldrich	Cat# C7880

(Continued on next page)



**Continued**

REAGENT or RESOURCE	SOURCE	IDENTIFIER
PBS 1X	GIBCO	Cat# 14190-094
HBSS 10X	GIBCO	Cat# 14180-046
FCS (Foetal Calf Serum) Eutroph®	Eurobio Scientific	Cat# CVFSVF00-01
EDTA acid disodium salt dihydrate	Sigma-Aldrich	Cat# E5134
DTT	Sigma-Aldrich	Cat# D9779-5G
Collagenase type IV	GIBCO	Cat# 17104-019
Collagenase type VIII	Sigma-Aldrich	Cat# C2139
DNase I, grade II, from bovine pancreas	Roche	Cat# 10104159001
Percoll	GE Healthcare	Cat# 17-0891-01
RPMI 1640 Medium, GlutaMAX Supplement	GIBCO	Cat# 61870-010
HEPES	GIBCO	Cat# 15630-056
Penicillin and Streptomycin (10,000 units/mL Penicillin and 10 mg/mL Streptomycin)	Sigma-Aldrich	Cat# P4333-100ML
2-Mercaptoethanol	Sigma-Aldrich	Cat# M3148-250ML
Red Blood Cell Lysing Buffer Hybri-Max	Sigma-Aldrich	Cat# R7757-100ML
Histopaque-1077	Sigma-Aldrich	Cat# 10771-500ML
GLPG 0974	Tocris	Cat# 5621
AR-C155858	Tocris	Cat# 4960
Trichostatin A (TSA)	Sigma-Aldrich	Cat# T8552-1MG
Sodium azide	Sigma-Aldrich	Cat# S2002-25G
Fixable Viability Dye eFluor 506	eBioscience	Cat# 65-0866-18
Zombie Aqua Fixable Viability Kit	BioLegend	Cat# 423101
PFA / Paraformaldehyde (formaldehyde) 32% Aqueous Solution	Electron Microscopy Sciences	Cat# 15714
Saponin	Sigma-Aldrich	Cat# 47036-50G-F
Formalin solution, neutral buffered, 10%	Sigma-Aldrich	Cat# HT501128-4L
PMA / Phorbol 12-myristate 13-acetate	Sigma-Aldrich	Cat# P1585-1MG and P8139-1MG
Ionomycin	Sigma-Aldrich	Cat# I3909-1ML and I9657-1MG and I0634-1MG
Brefeldin-A	Sigma-Aldrich	Cat# B7651-5MG
Mouse IL-23 recombinant protein	FisherSci / eBioscience	Cat# 12750060 / 14-8231-63
Mouse IL-1 $\beta$ recombinant protein	R&D Systems	Cat# 401-ML-005 or 010
Mouse IL-10 recombinant protein	R&D Systems	Cat# 417-ML-005
Human IL-7 recombinant protein	eBioscience	Cat# 14-8079-80
Phosphotungstic acid hydrate	Sigma-Aldrich	Cat# P4006-250G
Nukol Capillary GC Column	Supelco	Cat# 25326
2-Ethylbutyric acid	Sigma-Aldrich	Cat# 109959-100ML
SuperScript II Reverse Transcriptase	Invitrogen	Cat# 10328062
SuperScript IV VILO Master Mix	Invitrogen	Cat# 11756050
Takyon ROX SYBR MasterMix blue dTTP	Eurogentec	Cat# UF-RSMT-B0701
Luna Universal qPCR Master Mix	New England Biolabs	Cat# M3003E
Tween 20	Sigma-Aldrich	Cat# P1379-1L
H <sub>2</sub> SO <sub>4</sub> / Sulfuric acid 95.0-97.0%	VWR Chemicals	Cat# 20700.298P

**Critical commercial assays**

FOXP3 Fix/Perm Buffer Set	BioLegend	Cat# 421403
FoxP3 / Transcription factor Staining Buffer Set	Invitrogen	Cat# 00-5523
RNeasy Micro Kit	QIAGEN	Cat# 74004
RNeasy Mini Kit	QIAGEN	Cat# 74104
High-Capacity cDNA Reverse Transcription Kit	Applied Biosystems	Cat# 10400745

(Continued on next page)

**Continued**

REAGENT or RESOURCE	SOURCE	IDENTIFIER
LunaScript RT SuperMix Kit	New England Biolabs	Cat# E3010L
Mouse IL-17A (homodimer) Uncoated ELISA	Invitrogen	Cat# 88-7371
<b>Experimental models: Organisms/strains</b>		
Mouse: C57BL/6JRj (7-9-week-old females)	Janvier Labs	RRID:MGI:5752053
Mouse: C57BL/6JRj germ-free (5-week-old females)	Anaxem (Micalis, INRAE Jouy-En-Josas)	N/A
Mouse: FFAR2 <sup>-/-</sup>	Maslowski et al., 2009	N/A
Mouse: IL-10 <sup>-/-</sup>	IERP (INRAE Jouy-En-Josas)	N/A
<b>Oligonucleotides</b>		
See <a href="#">Table S1</a>		
<b>Software and algorithms</b>		
FlowJo	BD Biosciences	<a href="https://www.flowjo.com/">https://www.flowjo.com/</a>
OpenLab ChemStation (C.01.06)	Agilent	N/A
GraphPad Prism	GraphPad Software	<a href="https://www.graphpad.com/">https://www.graphpad.com/</a>

**RESOURCE AVAILABILITY**

**Lead contact**

Further information and requests for resources and reagents should be directed to and will be fulfilled by the Lead Contact, Marie-Laure Michel ([marie-laure.michel@inrae.fr](mailto:marie-laure.michel@inrae.fr)).

**Materials availability**

This study did not generate new unique reagents.

**Data and code availability**

The published article includes all datasets generated or analyzed during this study.

**EXPERIMENTAL MODEL AND SUBJECT DETAILS**

**Mouse models**

C57BL/6J mice (7-9-week-old females) were purchased from Janvier Labs. Ffar2<sup>-/-</sup> mice on C57BL/6J background were obtained from Pasteur Institute (Lille). IL-10<sup>-/-</sup> mice on C57BL/6J background were bred in-house (IERP, Jouy-En-Josas). All conventional mice were bred and maintained under specific pathogen-free conditions.

Germ-free (GF) mice (C57BL/6J WT) were obtained locally from the GF rodent breeding facility Anaxem (Germ-free animal facilities of the Micalis Institute, INRAE, France).

All animal experiments were done according to institutional guidelines approved by the local ethical panel and the Ministère de l'Éducation Nationale, de l'Enseignement Supérieur et de la Recherche, France (APAFIS#9154-201608231549742).

**Human subjects**

All individuals with IBD (age 27-61; female 4, male 9) were recruited in the Gastroenterology Department of the Saint Antoine Hospital (APHP, Paris, France) and provided informed consent. Approval for human studies was obtained from the local ethics committee (Comité de Protection des Personnes Ile-de-France IV, IRB 00003835 Suivitheque study; registration number 2012/05NICB).

**METHOD DETAILS**

**Antibiotic and SCFA treatment**

Mice were treated with either sodium propionate (200 mM, Sigma-Aldrich), sodium acetate (200 mM, Sigma-Aldrich) or sodium butyrate (100 mM, Sigma-Aldrich) in the drinking water for 3 weeks *ad libitum*. Solutions were prepared and changed every two or three days.

For antibiotic treatment, mice were treated with vancomycin (500 mg/L, Mylan), colistin (1 g/L, Sigma-Aldrich) or a broad-spectrum cocktail (ampicillin 1 g/L Euromedex, neomycin 1 g/L Euromedex, metronidazole 1 g/L Toku-e and vancomycin 500 mg/L Mylan) in

the drinking water supplemented with sucrose (10 g/L, Sigma-Aldrich) for 3 weeks. Fluid intake was monitored and the antibiotic solution was changed every two or three days.

In some experiments, SCFAs and vancomycin were administered together via the drinking water for 3 weeks.

### DSS-induced colitis model

To induce colitis, mice were administered drinking water supplemented with 2% DSS (MP Biomedicals) for 7 days, and then allowed to recover by drinking supplemented water for the next 2 days. The propionate was added in the drinking water 1 week before DSS administration and until euthanasia. Animals were monitored daily for weight loss.

### Germ-free (GF) experiment

Fresh stool samples from conventional mice were immediately transferred to an anaerobic chamber, in which the stool samples were suspended and diluted in LYHBHI medium (Liquid Brain-Heart Infusion (BD) with Yeast Extract (BD) and Hemine (Sigma-Aldrich)) supplemented with cysteine (0.5 mg/mL, Sigma-Aldrich). These fecal suspensions were used to inoculate mice. C57BL/6 GF mice (5-week-old females; Anaxem, Jouy-en-Josas) were inoculated via oral gavage with 250  $\mu$ L of fecal suspension (1:100) on two consecutive days. Experiments on GF mice were performed four weeks after inoculation.

### Cell preparation

For isolation of lamina propria immune cells, small intestine between stomach and cecum, cecum or colon between cecum and anal verge were cut out and open longitudinally. Tissues were washed with cold PBS 1X to remove the fecal and then were cut cross-sectionally into 0.5-1 cm long pieces and then mixed with 5 mL pre-warmed HBSS 1X with 5% FCS, EDTA (5 mM, Sigma-Aldrich) and DTT (0.145 mg/mL, Sigma-Aldrich) in the shaker at 37°C for 20 min. The supernatants were discarded and pellets were washed with cold PBS 1X. The tissue pieces were then transferred to a new tube and digested with collagenase type IV (680 U/mL, GIBCO) or collagenase type VIII (0.5 mg/mL, Sigma-Aldrich) supplemented with DNase I (1 mg/mL, Roche) for 30 or 20 min, respectively. All the contents were passed through a 100  $\mu$ m cell strainer. LPLs were obtained using the 40/80 Percoll centrifugation (GE Healthcare). Cells were centrifuged briefly and suspended in complete RPMI containing 10% (vol/vol) FCS (Eurobio Scientific), 1% HEPES (GIBCO), 100 U/mL Penicillin and 100  $\mu$ g/mL Streptomycin (Sigma-Aldrich) and 50  $\mu$ M 2-Mercaptoethanol (Sigma-Aldrich).

Mouse lymph nodes and spleen preparation: lymph nodes (axillary, brachial, and inguinal) and spleen were homogenized and washed in complete RPMI. For the spleen, erythrocytes were lysed with red blood cell lysing buffer (Sigma-Aldrich).

### Human PBMCs isolation

Heparinized whole blood was diluted with PBS 1:1, layered over Histopaque-1077 (Sigma-Aldrich) and centrifuged at 400g for 20 min without brake at room temperature. The peripheral blood mononuclear cell (PBMC) fraction was then washed in cold PBS and used for *in vitro* culture assays.

### In vitro culture assays

Murine cells were treated 4h *in vitro* with sodium propionate (10 mM), sodium butyrate (0.5 mM), sodium acetate (10 mM) or a mixture of the three SCFAs (10 mM in total: acetate 6 mM + butyrate 2mM + propionate 2mM). SCFAs were purchased from Sigma-Aldrich. To study the mechanisms of action, sodium propionate was added with or without MCT inhibitor (AR-C155858; 4  $\mu$ M, Tocris), GPR43 receptor inhibitor (GLPG 0974; 100  $\mu$ M, Tocris) and a selective and reversible hydroxamate inhibitor of class I and II HDACs (trichostatin A (TSA); 1  $\mu$ M, Sigma-Aldrich). To understand the role of IL-10, cells were treated 4h with recombinant mouse IL-10 protein (20 ng/mL, R&D systems).

Sorted  $\gamma\delta$  T cells were treated with sodium propionate (1mM) for 18h. For cell proliferation assay, cells were incubated for 4 days with IL-7 (20 ng/mL; eBioscience) with or without sodium propionate (1 mM).

Human PBMC were cultured in the presence of sodium propionate (1 mM), or a mixture of the three SCFAs (1 mM in total: acetate 0.6 mM, butyrate 0.2 mM, propionate 0.2 mM) for 18h.

### Flow cytometry and cell sorting

Flow cytometry was carried out by using LSRII (BD), LSR Fortessa X-20 (BD) or FACS Aria machines (BD). Single cell suspensions were prepared in FACS buffer: PBS 1X (GIBCO) supplemented with 2% (vol/vol) FCS (Eurobio Scientific), 0.01% (vol/vol) sodium azide (Sigma-Aldrich). Cells were stained on ice in PBS 1X (GIBCO) with Fixable Viability Dye eFluor 506 (eBioscience) or Zombie Aqua Fixable Viability Kit (BioLegend). Cells were surface stained in FACS buffer with the following antibodies; from eBioscience: APC-labeled anti-TCR $\gamma\delta$  (GL3), FITC-labeled anti-mouse CD3 $\epsilon$  (145-2C11), anti-CD16/32 (93); from BioLegend: BV785-labeled anti-mouse CD4 (RM4-5), BV605-labeled anti-mouse CD8 $\alpha$  (53-6.7), BV421-labeled anti-mouse CD27, BV711-labeled anti-human CD3 $\epsilon$  (UCHT1), AF700-labeled anti-human CD4 (RPA-T4), BV605-labeled anti-human CD8 $\alpha$  (RPA-T8), AF647-labeled anti-human TCR $\gamma\delta$  (B1), PE-labeled anti-human TCR V $\alpha$ 7.2 (3C10), BV785-labeled anti-human CD161 (HP-3G10). Cells were washed in FACS buffer before analysis. In mouse,  $\gamma\delta$  T cells are CD3<sup>+</sup>TCR $\gamma\delta$ <sup>+</sup> CD4<sup>-</sup> CD8<sup>-</sup>. In human,  $\gamma\delta$  T cells are CD3<sup>+</sup>TCR $\gamma\delta$ <sup>+</sup> and MAIT cells are CD3<sup>+</sup> TCR V $\alpha$ 7.2<sup>+</sup> CD161<sup>high</sup>.

After surface staining, cells were fixed using 4% (vol/vol) PFA (Electron Microscopy Sciences) in PBS 1X. Cells were permeabilized in FACS Buffer supplemented with 0.5% (wt/vol) saponin (Sigma-Aldrich). Intracellular staining was performed in the same permeabilization buffer with the following antibodies; from eBioscience: eF450-labeled anti-IL-17 (17B7), PE/Cy7-labeled anti-IFN- $\gamma$  (XMG1.2); from BioLegend: PE-labeled anti-IL-22 (Poly5164), PB-labeled anti-human IL-17 (BL168), PE/Cy7-labeled anti-human IL-22 (2G12A41), APC/Fire750-labeled anti-human IFN- $\gamma$  (4S.B3).

We performed mouse intracellular staining for ROR- $\gamma$ t and Ki67 according to the manufacturers' instructions (FOXP3 Fix/Perm Buffer Set, BioLegend or FoxP3/Transcription factor Staining Buffer Set, eBioscience) and with PE-labeled anti-ROR- $\gamma$ t (AFKJS-9) (eBioscience) or FITC-labeled anti-mouse Ki67 (BD PharMingen).

For intracellular analysis, mouse cells were first stimulated in culture medium containing 50 ng/mL PMA (Sigma-Aldrich) and 1  $\mu$ g/mL ionomycin (Sigma-Aldrich) for 3–4 h at 37°C, 5% CO<sub>2</sub>, in the presence of 10  $\mu$ g/mL Brefeldin-A (Sigma-Aldrich), 20 ng/mL mouse IL-23 recombinant protein (FisherSci/eBioscience) and 10 ng/mL mouse IL-1 $\beta$  recombinant protein (R&D Systems). For human cells, they were first stimulated in culture medium containing 50 ng/mL PMA (Sigma-Aldrich) and 1  $\mu$ g/mL ionomycin (Sigma-Aldrich) for 5–6 h at 37°C, 5% CO<sub>2</sub>, in the presence of 10  $\mu$ g/mL Brefeldin-A (Sigma-Aldrich).

Data were analyzed by using FlowJo software (BD Biosciences).

### SCFA analysis in cecal samples

Samples of cecal contents were water-extracted (2 vol/wt) and proteins were precipitated with 10% (vol/vol) phosphotungstic acid (Sigma-Aldrich). SCFAs of acidified supernatant (0.3  $\mu$ L) were separated on a gas chromatograph (Agilent Technologies) equipped with a split-splitless injector, a flame-ionisation detector and a Nukol capillary GC column (15 m X 0.53 mm, 0.5  $\mu$ m; Supelco) impregnated with SP-1000 (FSCAP Nukol; Supelco, Saint-Quentin-Fallavier, France). Hydrogen carrier gas flow rate was 10 mL/min and inlet, column and detector temperatures were 200, 100 and 240°C, respectively. 2-Ethylbutyrate (Sigma-Aldrich) was used as the internal standard. Samples were analyzed in duplicate. Data were collected and peaks integrated using the OpenLab ChemStation C.01.06 software (Agilent).

### RNA expression analysis

Total RNA was isolated with RNeasy Micro Kit or Mini Kit (QIAGEN) as per manufacturer's instructions. RNA was reverse transcribed in cDNA with SuperScript II Reverse Transcriptase (Invitrogen) by random hexamers (from High-Capacity cDNA Reverse Transcription Kit, Applied Biosystems) or with LunaScript RT SuperMix Kit (New England Biolabs) or with SuperScript IV VIL0 Master Mix (Invitrogen). Quantitative PCR was performed with Takyon ROX SYBR MasterMix blue dTTP (Eurogentec) or Luna Universal qPCR Master Mix (New England Biolabs) on StepOne equipment (Applied Biosystems). Relative expression is displayed in arbitrary units normalized to GAPDH via  $\Delta\Delta$ Ct method. Primer sequences are available in the [Table S1](#).

### Cytokine quantification

LPLs from cecum were prepared as above.  $1 \times 10^5$  cells (at  $1 \times 10^6$  cells/mL) per 96-well plate (CellStar) were stimulated in culture medium with 50 ng/mL PMA (Sigma-Aldrich) and 1  $\mu$ g/mL ionomycin (Sigma-Aldrich) with or without sodium propionate (1 mM), for 24 h at 37°C, 5% CO<sub>2</sub>, in the presence of 20 ng/mL mouse IL-23 recombinant protein (FisherSci/eBioscience) and 10 ng/mL mouse IL-1 $\beta$  recombinant protein (R&D Systems). The culture supernatants were frozen at –20°C until processing. ELISAs were performed on the supernatants to quantify the mouse IL-17A cytokine according to the manufacturer's instructions (Invitrogen) with Tween 20 (Sigma-Aldrich) and H<sub>2</sub>SO<sub>4</sub> (VWR Chemicals).

### QUANTIFICATION AND STATISTICAL ANALYSIS

Results are expressed as the mean  $\pm$  standard error of the mean (SEM). All statistical analysis was performed using GraphPad Prism 6 software, using two-tailed Man-Whitney test or Wilcoxon test to compare two groups; and ordinary one-way ANOVA or Friedman test to compare 3 groups. Correlation significance was determined using linear regression. \*,  $p < 0.05$ ; \*\*,  $p < 0.01$ ; \*\*\*,  $p < 0.001$ . n represents the number of mice or patients with IBD per group. Statistical details of experiments and exact value of n can be found in the figure legends.

**Supplemental information**

**Gut microbiota-derived short-chain fatty acids  
regulate IL-17 production by mouse  
and human intestinal  $\gamma\delta$  T cells**

**Louise Dupraz, Aurélie Magniez, Nathalie Rolhion, Mathias L. Richard, Grégory Da Costa, Sothea Touch, Camille Mayeur, Julien Planchais, Allison Agus, Camille Danne, Chloé Michaudel, Madeleine Spatz, François Trottein, Philippe Langella, Harry Sokol, and Marie-Laure Michel**



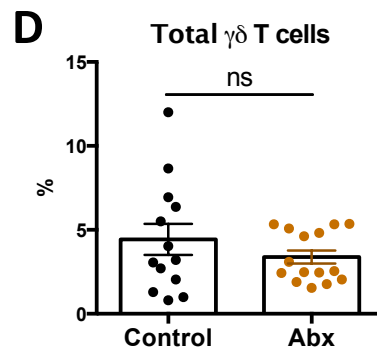
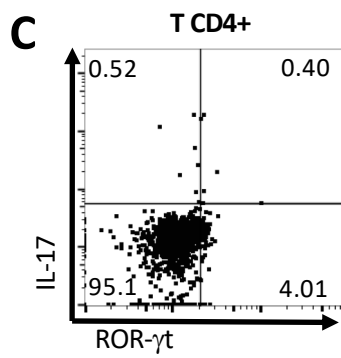
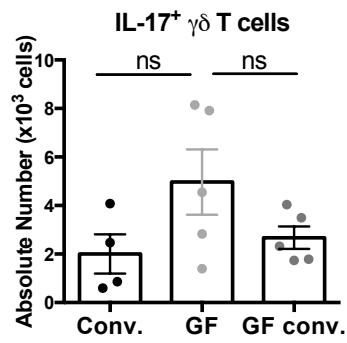
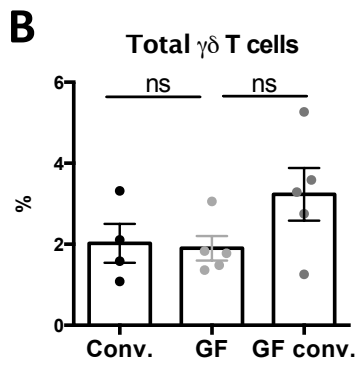
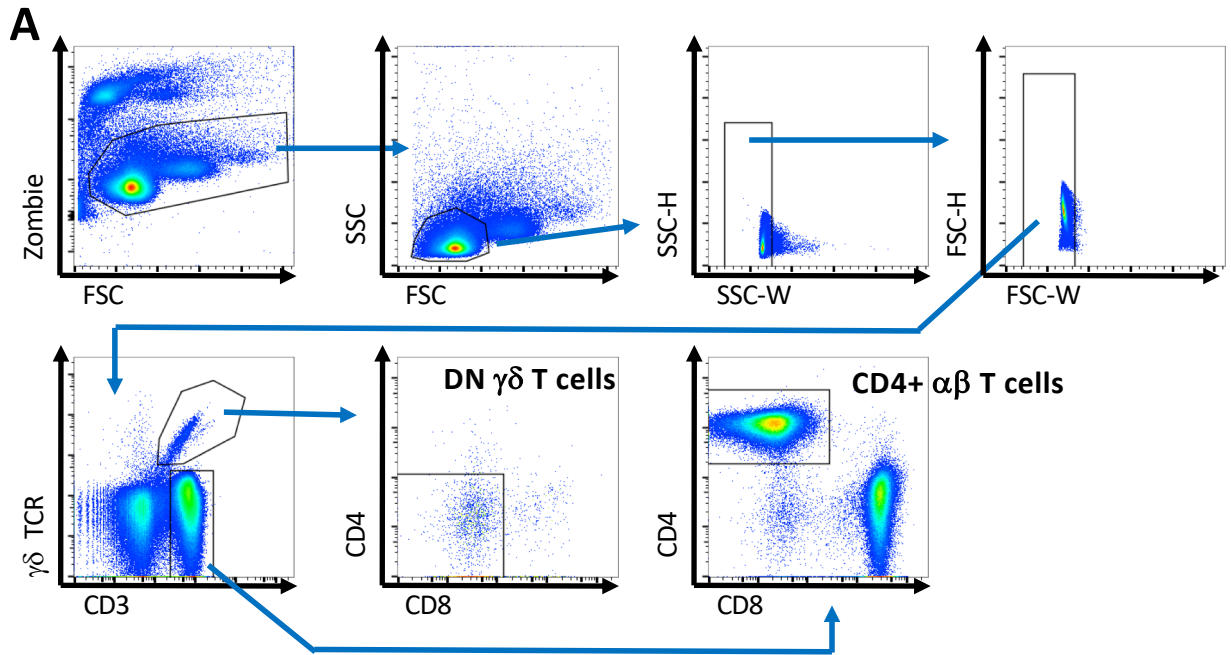


**Figure S1. Gut microbiota regulates differentially cecal  $\gamma\delta$  T cells.** Related to Figure 1

(A) Flow cytometry gating strategy used to identify CD4<sup>-</sup> CD8<sup>-</sup> (DN)  $\gamma\delta$  T cells and CD4<sup>+</sup>  $\alpha\beta$  T cells.

(B) Representative plots of total  $\gamma\delta$  T cells and absolute number of IL-17<sup>+</sup>  $\gamma\delta$  T cells from cecum obtained from untreated conventional mice (Conv.), germ-free mice (GF) and germ-free mice colonized with conventional mouse microbiota for 4 weeks (GF conv.).

(C) Intracellular analysis of IL-17 and ROR- $\gamma$ t expression by gated  $\alpha\beta$  CD4<sup>+</sup> T cells from cecum obtained from germ-free mice. Representative plot from n = 5. Numbers indicate percent of cells in relevant quadrant.

(D) Representative plots of total  $\gamma\delta$  T cells from cecum obtained untreated mice (Control) and broad spectrum antibiotics-treated mice (Abx).

In each case, cells were stimulated with PMA + Ionomycin + IL-1 $\beta$  + IL-23 for 3h. For all plots, numbers indicate percent of cells in relevant quadrant. Error bars are SEM from 13-15 mice (D) per group. Significant differences were determined using two-tailed Mann-Whitney test; ns=non significant.

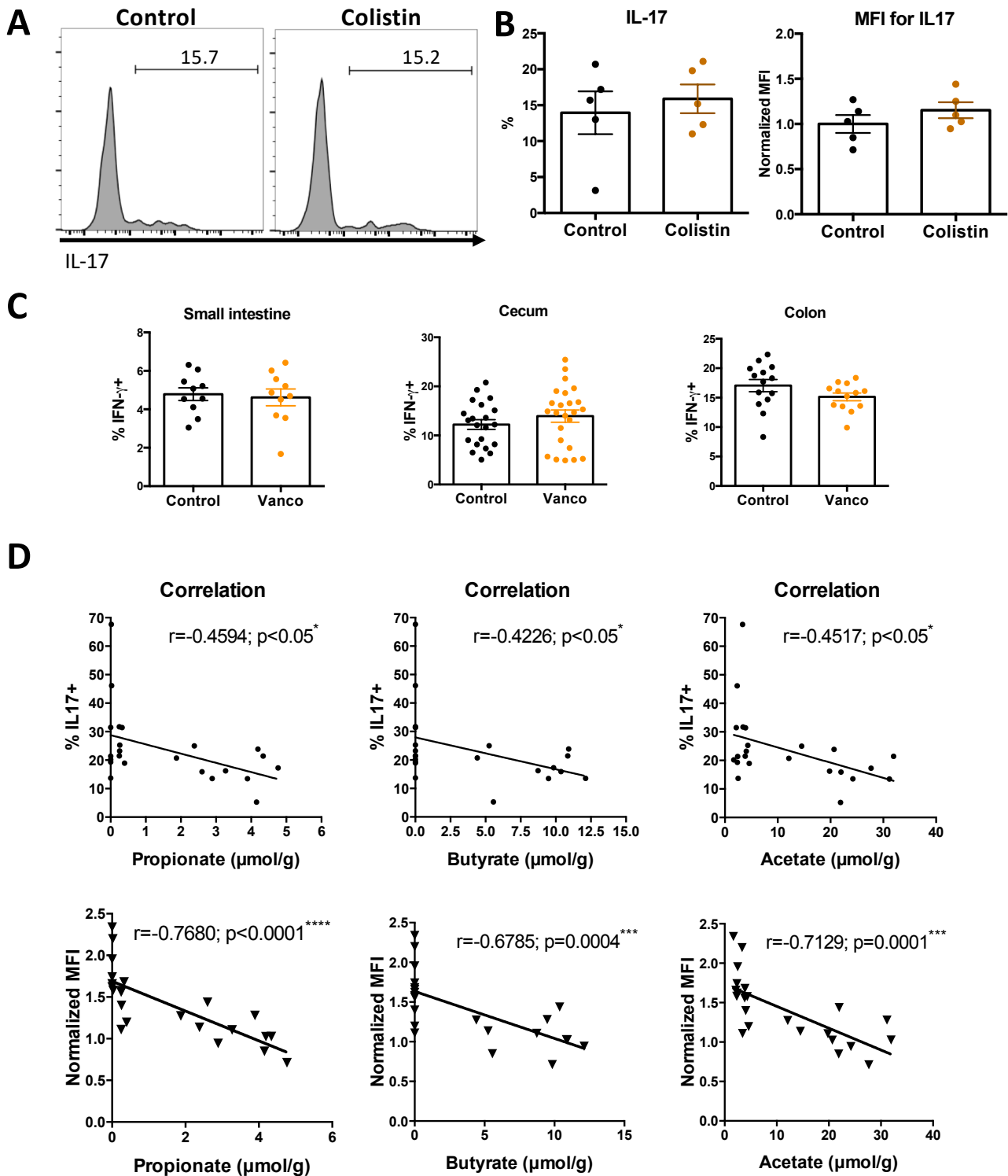


**Figure S2. Gut microbiota regulates differentially cecal  $\gamma\delta$  T cells.** Related to Figure 2.

(A) Intracellular analysis of IL-17 expression by gated  $\gamma\delta$  T cells from cecum obtained from untreated mice (Control) and colistin-treated mice.

(B) IL-17 production and normalized median fluorescence intensity (MFI) for IL-17 (middle) in gated  $\gamma\delta$  T cells by cecal  $\gamma\delta$  T cells obtained as in (A).

(C) Intracellular analysis of IFN- $\gamma$  expression by gated  $\gamma\delta$  T cells from small intestine (left), cecum (middle) and colon (right) obtained from untreated mice (Control, black) and vancomycin-treated mice (Vanco, grey).

(D) Spearman correlation between propionate, butyrate and acetate concentrations and IL-17 production (percentage, up or median fluorescence intensity, bottom) in gated  $\gamma\delta$  T cells from cecum obtained from untreated mice and antibiotic-treated mice (vancomycin, colistin or 4 Abx).

In each case, cells were stimulated with PMA + Ionomycin + IL-1 $\beta$  + IL-23 for 3h. Error bars are SEM from 5 mice (A and B), 10-24 mice per group (C) and 23 mice (D).

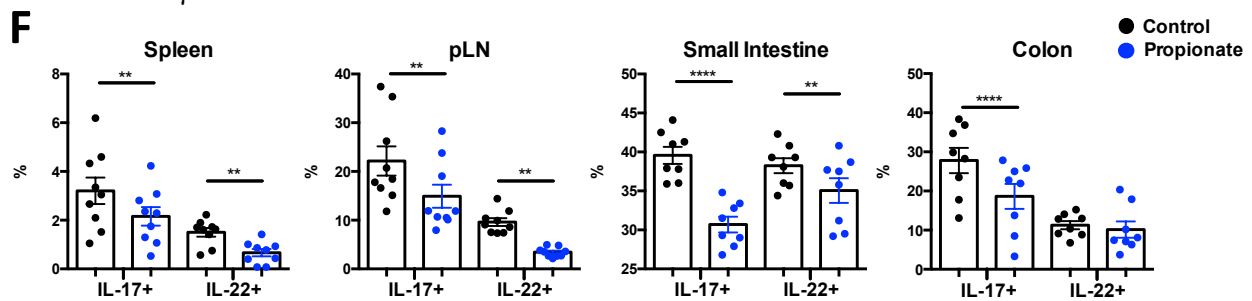
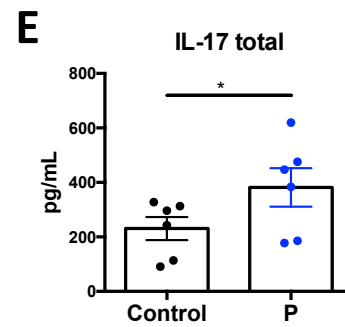
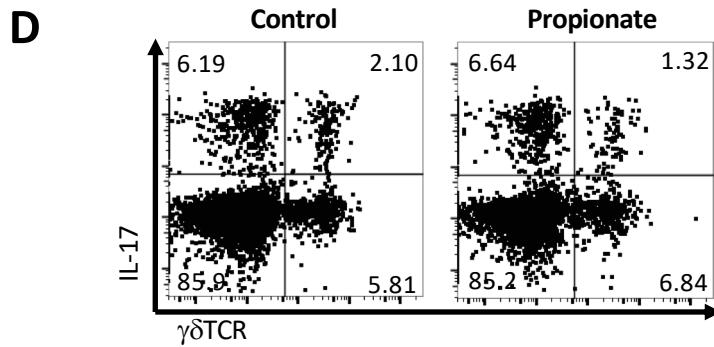
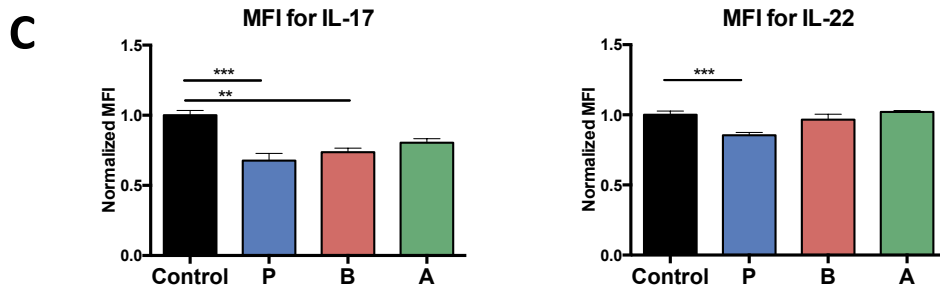
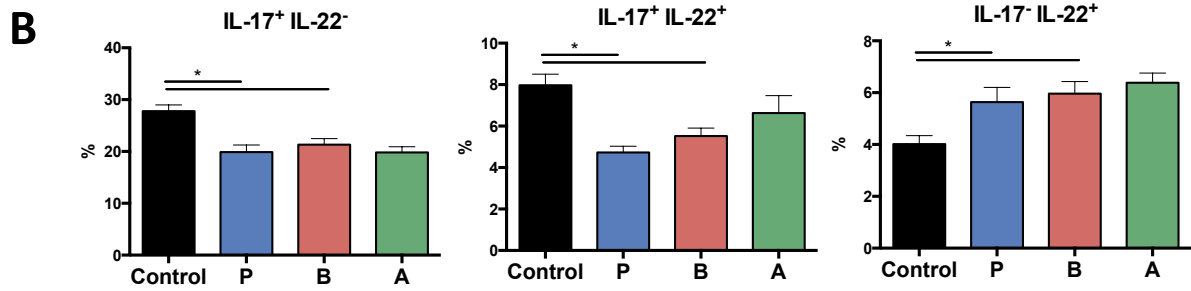
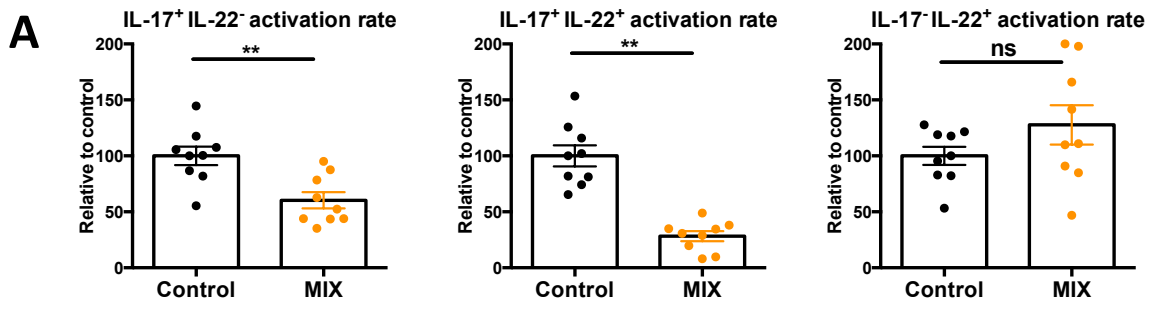


**Figure S3. SCFAs inhibit IL-17 and IL-22 productions by  $\gamma\delta$  T cells.** Related to Figure 3.

(A-B) Intracellular analysis of gated IL-17<sup>+</sup> IL-22<sup>-</sup> (left), IL-17<sup>+</sup> IL-22<sup>+</sup> (middle), IL-17<sup>-</sup> IL-22<sup>+</sup> (right)  $\gamma\delta$  T cells from cecum cultured for 4h with PBS (Control), a mix of propionate, butyrate and acetate (SCFA mix) (A) or propionate, butyrate or acetate (B). Cells were stimulated with PMA + Ionomycin + IL-1 $\beta$  + IL-23 for the last 3h. A, acetate; B, butyrate; P, propionate

(C) Normalized median fluorescence intensity for IL-17 and IL-22 in gated  $\gamma\delta$  T cells from cecum obtained as described in B. A, acetate; B, butyrate; P, propionate

(D) Representative plots of CD3<sup>+</sup> T cells from cecum cultured for 4h with PBS (Control) or propionate and activated as in B. For all plots, numbers indicate percent of cells in relevant quadrant.

(E) Total cecum were stimulated *in vitro* by PMA + Ionomycin + IL-1 $\beta$  + IL-23 in the presence (P) or absence (Control) of propionate during 24h. IL-17 levels were measured in supernatants. P, propionate

(F) Intracellular analysis of IL-17 and IL-22 expression by gated  $\gamma\delta$  T cells from small intestine, colon, spleen and peripheral lymph nodes (pLN) cultured for 4h with PBS (Control) or propionate. Cells were stimulated with PMA + Ionomycin + IL-1 $\beta$  + IL-23 for the last 3h.

Error bars are SEM from 9 mice (A), 7-8 mice (B-C), 6 mice (E) and 8-9 mice (F) per group. Significant differences were determined using two-tailed Wilcoxon test; \*P < 0.05, \*\*P < 0.01, \*\*\*\*P < 0.0001.



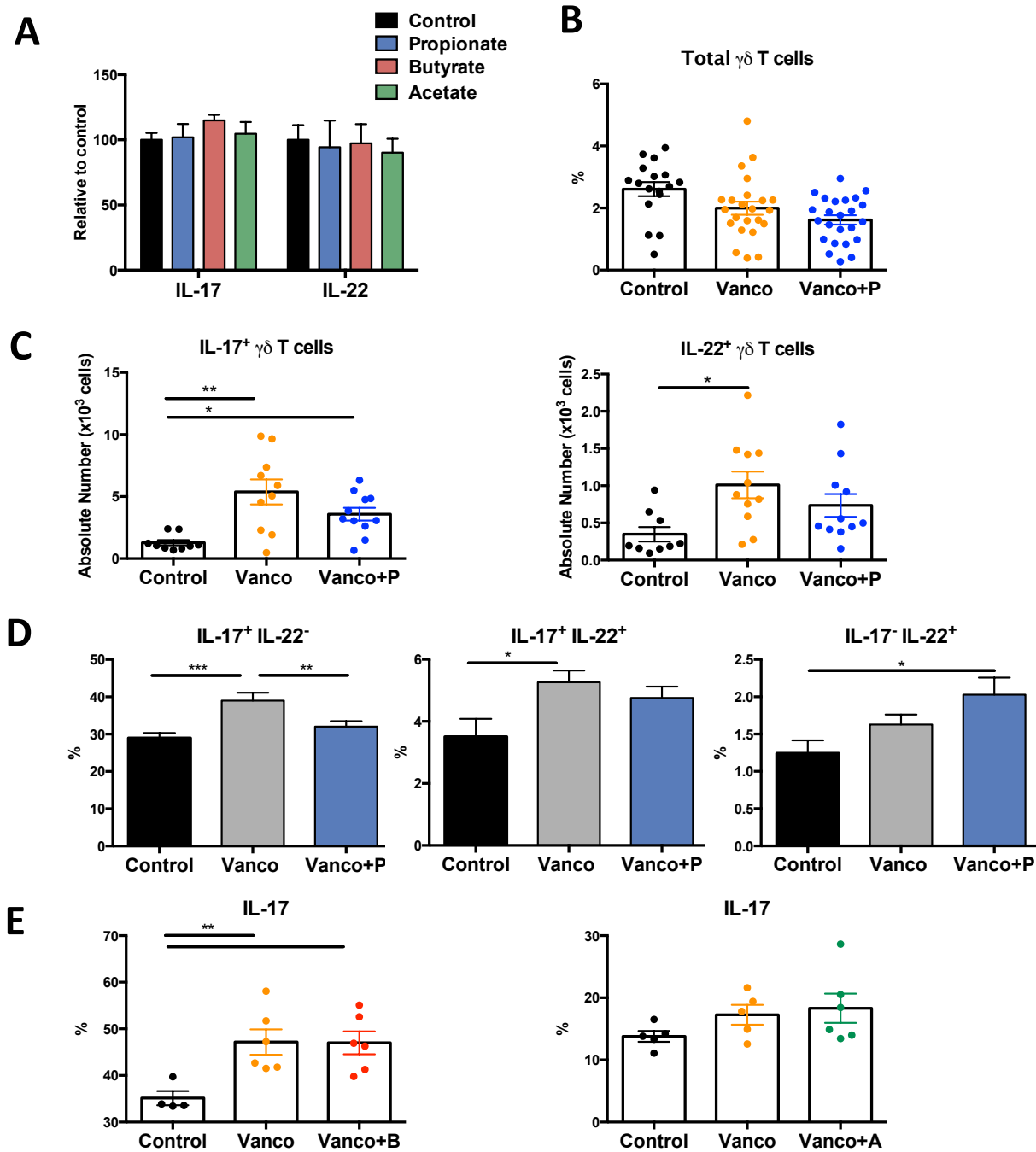


**Figure S4. Butyrate and Acetate do not inhibit IL-17 and IL-22 productions by  $\gamma\delta$  T cells from antibiotic-treated mice.** Related to Figure 4.

(A) Production of IL-17 and IL-22 expression by gated  $\gamma\delta$  T cells from cecum obtained from mice treated with propionate, butyrate or acetate, in comparison to control group.

(B-C) Representative plots of total  $\gamma\delta$  T cells (B) and absolute number of IL-17<sup>+</sup> and IL-22<sup>+</sup>  $\gamma\delta$  T cells (D) from cecum obtained from untreated mice (Control), vancomycin-treated mice (Vanco) and mice treated with vancomycin and propionate (Vanco+P). P, propionate

(D) Intracellular analysis of gated IL-17<sup>+</sup> IL-22<sup>-</sup> (left), IL-17<sup>+</sup> IL-22<sup>+</sup> (middle), IL-17<sup>-</sup> IL-22<sup>+</sup> (right)  $\gamma\delta$  T cells from cecum obtained as in (B). P, propionate

(E) Intracellular analysis of IL-17 expression by gated  $\gamma\delta$  T cells from cecum obtained from untreated mice (Control), vancomycin-treated mice (Vanco) and mice treated with vancomycin and butyrate (Vanco+B) or acetate (Vanco+A).

In each case, cells were stimulated with PMA + Ionomycin + IL-1 $\beta$  + IL-23 for the last 3h. B, butyrate; A, acetate. Error bars are SEM from 5-10 mice (A), 17-24 mice (B and D), 9-11 mice (C) and 4-6 mice (E) per group. Significant differences were determined using one-way analysis of variance (ANOVA); \*P < 0.05, \*\*P < 0.01, \*\*\*P < 0.001.

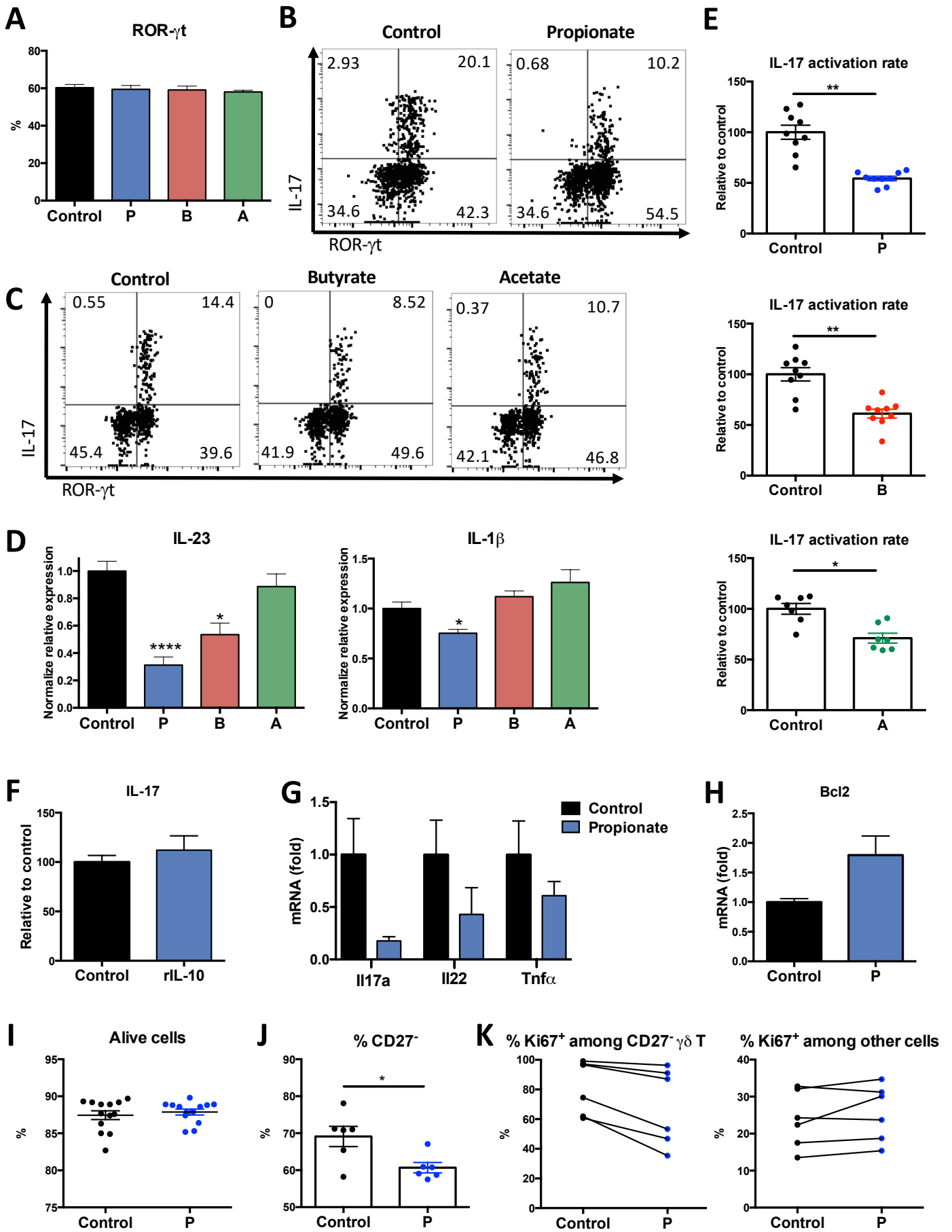


**Figure S5. The effect of propionate on  $\gamma\delta$  T cells is not dependent to IL-1 $\beta$ , IL-23 or IL-10.** Related to Figure 5.

(A) Intracellular analysis of ROR- $\gamma$ t expression by gated  $\gamma\delta$  T cells from cecum cultured for 4h with PBS (Control), propionate, butyrate or acetate and activated with PMA + Ionomycin + IL-1 $\beta$  + IL-23 for the last 3h. Error bars are SEM. A, acetate; B, butyrate; P, propionate

(B-C) Representative plots of  $\gamma\delta$  T cells from cecum obtained as described in A. For all plots, numbers indicate percent of cells in relevant quadrant.

(D) IL23 and IL1 $\beta$  mRNA quantification by qPCR. Lamina propria cells from cecum cultured for 3h with PBS (Control), propionate, butyrate or acetate and activated with PMA + Ionomycin for the last 2h. A, acetate; B, butyrate; P, propionate

(E) IL-17 activation rate relative to control on gated  $\gamma\delta$  T cells from cecum cultured for 4h with PBS (Control), propionate, butyrate or acetate and activated with PMA + Ionomycin for the last 3h. A, acetate; B, butyrate; P, propionate

(F) IL-17 activation rate relative to control on gated  $\gamma\delta$  T cells from cecum cultured for 4h with PBS (Control), or rIL-10 and activated as in A.

(G) IL17a, IL22 and Tnf $\alpha$  mRNA quantification by qPCR in sorted  $\gamma\delta$  T cells from cecum cultured 3h with PBS (Control) or propionate and activated with PMA + Ionomycin + IL-1 $\beta$  + IL-23 for the last 2h. Error bars are SEM.

(H) Bcl2 mRNA quantification by qPCR in sorted  $\gamma\delta$  T cells from cecum cultured 18h with PBS (Control) or propionate. P, propionate

(I) Proportion of alive cells from total lymph nodes cultured for 4h with PBS (Control) or propionate and activated with PMA + Ionomycin + IL-1 $\beta$  + IL-23 for the last 3h. P, propionate

(J) Proportion of CD27 $^-$  cells among gated  $\gamma\delta$  T cells from LN cells cultured for 4 days with IL-7 (Control) or IL-7 + propionate. P, propionate

(K) Proportion of Ki67 $^+$  (cells in cycle) in gated CD27 $^-$   $\gamma\delta$  T cells and TCR $\delta$  $^-$  cells from LN treated as in (J). P, propionate

Error bars are SEM from 5-7 mice (A), 7-9 mice (E), 3 mice (F-G), 4 mice (H), 13 mice (I) and 6 mice (J-K) per group. Significant differences were determined using two-tailed Wilcoxon test; \*P < 0.05, \*\*P < 0.01.

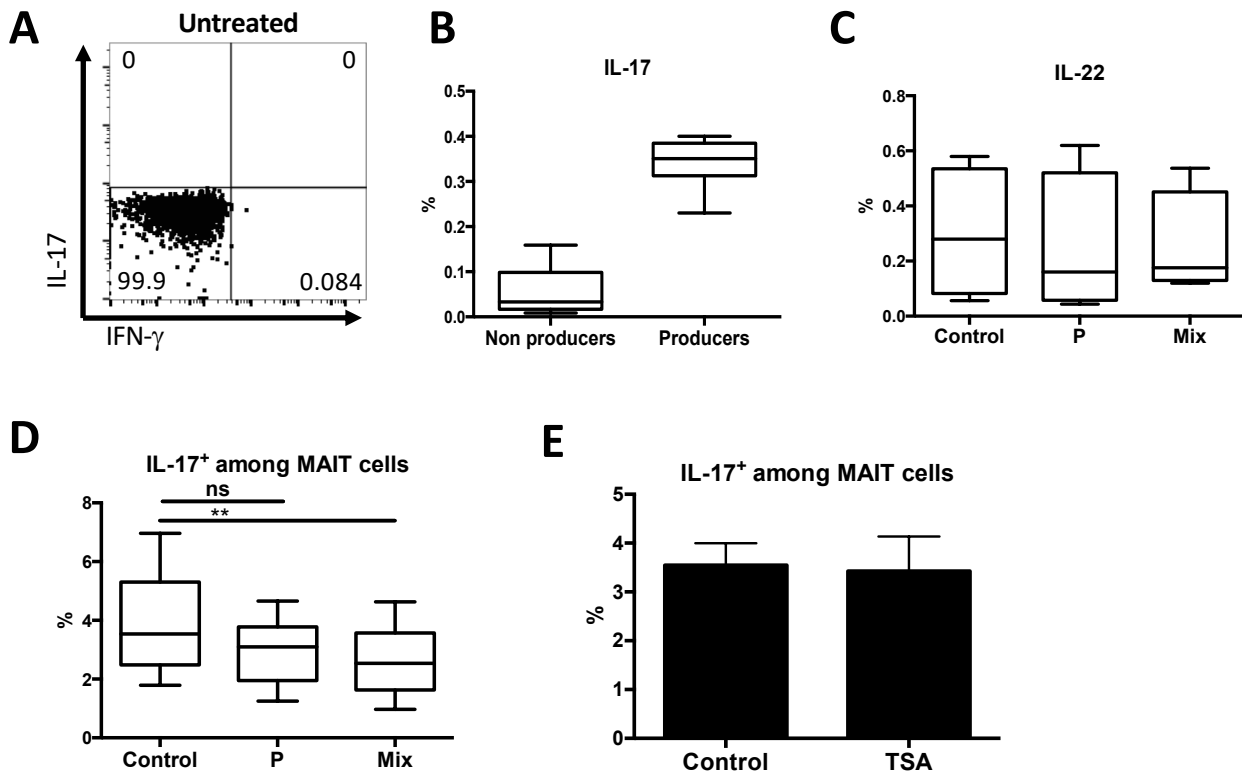


**Figure S6. SCFAs inhibit specifically IL-17 production by human  $\gamma\delta$  T cells.** Related to Figure 6.

(A) Intracellular analysis of IL-17 and IFN- $\gamma$  expression by gated  $\gamma\delta$  T cells from PBMC of IBD patients, untreated and without PMA + Ionomycin stimulation. For all plots, numbers indicate percent of cells in relevant quadrant.

(B) Collective analysis of IL-17 expression by  $\gamma\delta$  T cells from IBD patients, non-producers of IL-17 (<0.2%) and IL-17 producer (<0.2%), stimulated with PMA + Ionomycin for the last 5h; data are expressed as box plots. Each box represents the interquartile range (IQR). Lines inside the boxed represent the median. Whiskers represent the highest and lowest values.

(C-D) Collective analysis of IL-22 (C) and IL-17 (D) by gated  $\gamma\delta$  T cells (C) and MAIT cells (D) from IBD patients, untreated (Control), or treated 18h with propionate or a mix of SCFAs (Mix), and stimulated with PMA + Ionomycin for the last 5h; data are expressed as box plots. Each box represents the interquartile range (IQR). Lines inside the boxed represent the median. Whiskers represent the highest and lowest values. \*\*P < 0.005, versus control (Friedman-test). P, propionate

(E) IL-17 activation production by gated MAIT cells from IBD patients, treated 18h with PBS (Control) or TSA and activated with PMA + Ionomycin for the last 5h. Error bars are SEM from n = 8.

**Table S1. Oligonucleotides used in this study. Related to STAR Methods.**

REAGENT or RESOURCE	SOURCE	IDENTIFIER
Oligonucleotides		
GAPDH Forward 5'-AACTTTGGCATTGTGGAAGG-3' Reverse 5'-ACACATTGGGGGTAGGAACA-3'	Lamas et al., Nat Med, 2016	N/A
FFAR3 Forward 5'-CTTCTTTCTTGGCAATTACTGGC-3' Reverse 5'-CCGAAATGGTCAGGTTTAGCAA-3'	<a href="https://pga.mgh.harvard.edu/primerbank/">https://pga.mgh.harvard.edu/primerbank/</a>	N/A
FFAR2 Forward 5'-AATTCCTGGTGTGCTTTGG-3' Reverse 5'-ACCAGACCAACTTCTGGGTG-3'	Smith, Science, 2013	N/A
MCT1 Forward 5'-ATTGTGGAATGCTGCCCTGT-3' Reverse 5'-CGTCTCCTTTGGCTTCTCGT-3'	This paper	N/A
SMCT1 Forward 5'-CGGGACATCGGCAGTTTTG-3' Reverse 5'-CTGCGACCGCCATAAGAA-3'	<a href="https://pga.mgh.harvard.edu/primerbank/">https://pga.mgh.harvard.edu/primerbank/</a>	N/A
IL-23 Forward 5'-AGCGGGACATATGAATCTACTAAGAGA-3' Reverse 5'-GTCCTAGTAGGGAGGTGTGAAGTTG-3'	Cha et al., JI, 2010	N/A
IL-1 $\beta$ Forward 5'-GCCCATCCTCTGTGACTCAT-3' Reverse 5'-AGGCCACAGGTATTTTGTCTG-3'	Conway et al., JI, 2012	N/A
IL-17A Forward 5'-TTTAACTCCCTTGGCGCAAAA-3' Reverse 5'-CTTCCCTCCGCATTGACAC-3'	Lamas et al., Nat Med, 2016	N/A
IL-22 Forward 5'-CATGCAGGAGGTGGTGCCTT-3' Reverse 5'-CAGACGCAAGCATTCTCAG-3'	Tomkovich, Cancer Res, 2017	N/A
TNF- $\alpha$ Forward 5'-GACCCTCACACTCAGATCATCTTCT-3' Reverse 5'-CCACTTGGTGGTTTGCTACGA-3'	Li et al., Cent Eur J Immunol, 2014	N/A
BCL2 Forward 5'-TGAGTACCTGAACCGGCATCT-3' Reverse 5'-GCATCCAGCCTCCGTTAT-3'	Fachi, JEM, 2019	N/A